UNIVERSITY OF CALIFORNIA
RIVERSIDE

Advanced Eco-Driving for Connected and Automated Vehicles in Complex Traffic Scenarios

A Dissertation submitted in partial satisfaction
of the requirements for the degree of

Doctor of Philosophy

in

Electrical Engineering

by

Zhensong Wei

December 2023

Manuscript Committee:

Dr. Matthew J. Barth, Co-Chairperson
Dr. Peng Hao, Co-Chairperson
Dr. Hamed Mohsenian-Rad

The Dissertation of Zhensong Wei is approved:

Committee Co-Chairperson

Committee Co-Chairperson

University of California, Riverside

ABSTRACT OF THE DISSERTATION

Advanced Eco-Driving for Connected and Automated Vehicles in Complex Traffic Scenarios

by

Zhensong Wei

Doctor of Philosophy, Graduate Program in Electrical Engineering
University of California, Riverside, December 2023
Dr. Matthew J. Barth, Co-Chairperson
Dr. Peng Hao, Co-Chairperson

Transportation related activities has substantially increased the mobility of people and goods, but also brings impacts to the environment, such as greenhouse gas (GHG) emissions, air pollution, energy consumption, and health problems. This growing energy consumption and emission crisis has drawn tremendous attention from the public agencies, industry and researchers. Different solutions have been proposed to reduce the energy consumption from the transportation sector. For example, alternative energy sources, such as electricity and hydrogen, have been proposed as more energy-efficient and environmental-friendly fuel sources. In addition to eco-friendlier fuel sources, wireless communication and automated driving technology can also be applied to develop

connected eco-friendly transportation systems. Connected and automated vehicles (CAVs) have shown the capability to improve traffic mobility and energy efficiency via vehicle-to-vehicle (V2V) or vehicle-to-infrastructure (V2I) communication. Among all CAV applications, Eco Approach and Departure (EAD) at Signalized Intersections is particularly promising for fuel saving and emission reduction in urban area, as drivers would effectively reduce stops and idling and avoid unnecessary acceleration and deceleration by receiving signal timing information in advance.

In real-world traffic, signal timing and traffic conditions are quite dynamic and uncertain in the scope of different road networks. Due to the existence of different varieties of vehicle classes and vehicle engine types, the algorithm developed for eco-driving also needs to be powertrain-specific. In this dissertation, advanced eco-trajectory planning algorithms have been developed to address four challenges: 1) Driving in urban areas with uncertain queue conditions due to the limitation of the communication and sensing range; 2) Developing an adaptive Eco-Approach and Departure (EAD) strategy to minimize the expected energy consumption when passing an actuated signalized intersection; 3) Extending the intersection-based eco-driving algorithm to corridor level for global optimal performance; and 4) Customizing eco-driving algorithms to other vehicles, such as electric trucks, under different traffic volumes and vehicle fleet mix.

To solve those challenging but urgent issues in the EAD application, graph-based models have been created with nodes representing states of the host vehicle and traffic condition, and directed edges with weight representing expected energy consumption between two connected states. The shortest path is calculated that minimizes the total expected energy

consumption for vehicles approaching the signalized intersections. Machine learning techniques have been applied to generate an approximate solution from the graph-based model in order to reduce computation time. A comprehensive framework is designed for adaptive connected eco-driving strategy under mixed traffic conditions, which could be applied to different types of vehicles without sacrificing safety and mobility. An average energy savings of 9% and 24% have been reached for unknown queue and actuated signals, respectively, and an energy saving of 8.8% - 11.8% has been achieved for corridor eco-driving applications. When applied to battery electric trucks, an energy savings of 1.4% to 6.5% can be achieved while maintaining a similar travel time.

Contents

List of Figures

List of Tables

1. **Introduction**

1. 1 Background and Problem Statement

Transportation related activities has substantially increased the mobility of people and goods, but also brings impacts to the environment, such as greenhouse gas (GHG) emissions, air pollution, energy consumption, and health problems. As shown in Figure 1.1, according to the 2021 GHG emission report from the United States Environment Protection Agency, the transportation sector has become the largest contributor (28%) to the U.S. GHG emissions, surpassing the emission of its biggest competitor (electricity) for the first time in history (*1*). 81% of the gas was emitted by light-duty vehicles and medium/heavy-duty trucks, which makes them the two most dominant sectors of the six main mobile sources (*1*). According to the statistics from the U.S. Department of Energy, the energy consumption of transportation has kept increasing since 2020, reaching 27.5 quadrillion Btu (British thermal unit) and a share of 27.4% of the U.S. total energy consumption by end-use sector in 2022(*2*).

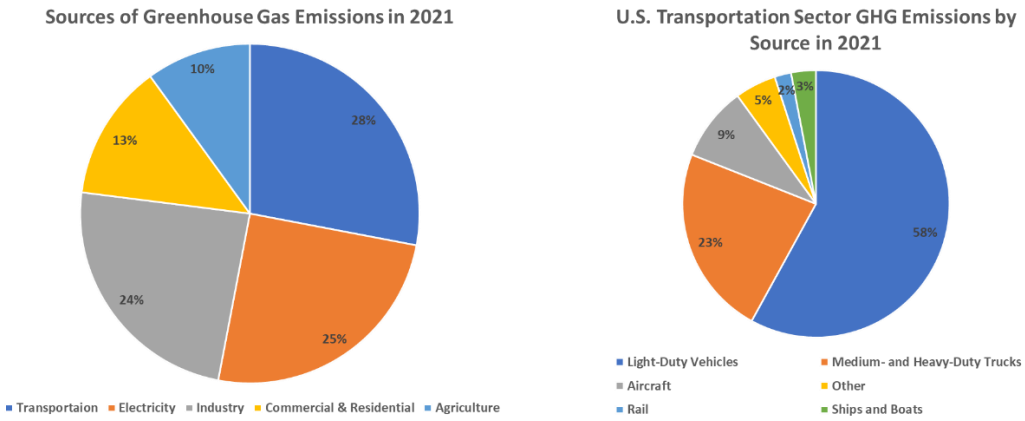

Figure 1.1. The U.S. Sources of Greenhouse Gas Emissions in 2021 (*1*)

The growing energy crisis and GHG emissions have drawn tremendous attention from government, car manufacturers, and researchers, and different solutions have been brought up to reduce the energy consumption of the transportation-related fields. Alternative energy sources, such as electricity and hydrogen, have been suggested as more energy-efficient and environmentally friendly fuel sources for zero-emission vehicles (ZEVs) including pure battery plug-in electric vehicles, plug-in hybrid electric vehicles, and hydrogen fuel cell electric vehicles. Established by the California Air Resources Board (CARB), the ZEV program is aiming to reach a total of 5 million ZEVs on the roads by 2030 and 250k charging stations by 2025 (3).

Besides these eco-friendlier fuel sources, wireless communication, and automated driving technology can also be applied to develop the connected eco-friendly transportation systems (*4*). Connected vehicles (CVs) have shown the capability to improve traffic mobility and energy efficiency via vehicle-to-vehicle (V2V) or vehicle-to-infrastructure (V2I) communication. Automated vehicles (AVs) equipped with sensing technology (e.g. camera, Lidar, radar, etc.) and artificial intelligent (AI) technology would recognize the environment and subsequently precisely perform eco-friendly actions by fully or partial automation. In Europe, starting from 2010, the project eCoMove has developed a transport energy efficiency system based on vehicle-to-vehicle (V2V) and vehicle-to-infrastructure (V2I/I2V) communication, where real-time data can be shared among the vehicles and traffic controllers supporting a more fuel-saving traffic system (*5*). In the U.S., Application for the Environment: Real-Time Information Synthesis (AERIS) research program established by the Intelligent Transportation Systems (ITS) Joint Program Office (JPO) in

2014 has developed 18 Connected and Automated Vehicle (CAV) applications for five operational scenarios, among which Eco-Approach and Departure (EAD) at Signalized Intersections has been validated to be an effective application in decreasing fuel consumption and emissions (*6*).

The EAD application in the host CV can calculate the most energy-efficient speed profile and guide the vehicle to pass the target traffic signal in an eco-friendly manner after collecting the Basic Safety Message (BSM) from other CVs and Signal Phase and Timing (SPaT) information transmitted from the roadside equipment unit (*12*). Unlike driving on freeways, the frequent stop-and-go maneuvers and associated accelerations due to the signal control and traffic result in excessive fuel consumption and air pollutant emissions. In real-world traffic, **signal timing** and **traffic** conditions usually appear to be dynamic and uncertain. For example, when a CV is approaching an actuated signalized intersection, the remaining time of the current signal phase indicated by the SPaT message can be updated dynamically. Meanwhile, the traffic-related information received from other CVs and radar is also highly uncertain due to the limited sensing range and varying driving behaviors of other vehicles. Therefore, the look-ahead signal timing and traffic condition of the downstream intersection is hard to predict, which brings challenges to develop applicable EAD models. Besides the SPaT messages and traffic condition (in particular the number of queued vehicles or queue length) that serve as a main requirement for the application, other types of information such as **geographic data** (road network) and **vehicle type/powertrain** also contribute to the calculation of an ideal speed profile. If the vehicle is driving on a signalized corridor, the SPaT information from the following

intersections could also be integrated together to reach a better performance. It is also critical to extend the existing EAD application (which is more focused on combustion engine-based passenger cars) to other vehicle types (e.g. medium and heavy-duty vehicle) and powertrains (e.g. electric vehicles and hybrid vehicles) by developing powertrain-specific EAD models. Therefore, the challenges remain on how to design safe, robust, and real-time capable eco-driving strategies in these complex traffic scenarios, with dynamic signal, traffic, road networks, and vehicle compositions.

1.2 Related Work

In the past decade, many EAD applications using SPaT information have been developed to calculate an energy-efficient vehicle speed profile for passing through intersections. Taking advantage of communication and sensing technology, the knowledge of SPaT information, map information, vehicle powertrain and dynamics, and preceding vehicle's state, different EAD applications have been developed for complex scenarios such as actuated signal and congested traffic (*7–11*). As shown in Table 1.1, in terms of formulated models, existing EAD models can be categorized into three classes: the rule-based model, learning-based model and the optimization model. Rule-based models are computationally efficient but do not guarantee the optimality of the solution (*9, 12–14, 25-26, 29*). Optimization models can find the optimal solution theoretically, but the actual performance is limited by the computation time and the difficulty to formulate an explicit energy-oriented objective function as most energy estimation models are non-polynomial, non-convex, and even non-equational (*11, 15–24, 28, 30-31*). Learning-based models can usually achieve similar performance as the optimization models in real-time, but the

performance is also restricted to the amount of data used for training (*27*). In terms of signal timing and traffic conditions, most research does not consider the uncertainty queue or signal actuation, which lead to the application work being less efficient under more complex scenarios. The total fuel saving is usually within 10-20% based on the different baselines these models are compared to.

In addition to the lack of adaptivity to the traffic and signal uncertainty on the road, the majority of the EAD applications have been developed based on a single intersection, in which the vehicle will only operate based on the SPaT information from the nearest signal. Hao et al. developed an eco-driving strategy for trucks and calibrated the system using real-world acceleration and deceleration profile data in microsimulation (*24*). Altan et al. designed a partially automated vehicle system with an EAD feature to automatically follow the recommended speed profiles and achieved an average fuel savings of 17% (*25*). Jiang et al. developed an EAD system for left-turn vehicles that could improve both mobility and fuel efficiency (*26*). In (*27*), a deep learning-based EAD for plug-in hybrid electric bus and a queue prediction model is further developed to address the effect of downstream traffic. Guo et al. proposed a model predictive control (MPC) strategy to find the energy-optimal torque split, gear shift, and velocity control of a hybrid electric vehicle (HEV) (*28*). Wan et al. employed a speed advisory system for CV in mixed traffic and found that SAS-equipped vehicles improve energy efficiency of conventional vehicles as well (*29*). Jiang et al. smoothed out the shock wave caused by signal controls and studied the energy benefits of EAD under different penetration rates (*30*). He et al. proposed a multi-stage optimal control problem to minimize vehicle fuel consumption considering the impacts of

Table 1.1. Summary of Connected Eco-Driving Models

Authors	Method	Model description	Corridor	Traffic	Signal Actuation	Fuel saving
Sindhura et al. (*15*)	Optimization	Acceleration rate minimization	Yes	No	No	14%
Li et al. (*12*)	Rule-based	Drivers make control based on alerts	No	No	No	8%
Asadi and Vahidi *(13)*	Rule-based	Predictive cruise control	No	No	No	59%
Barth et al. *(9)*	Rule-based	Trigonometric speed profiles	No	No	No	15%
Rakha et al. (*16)*	Optimization	Fuel as the optimization objective	No	Yes	No	25%
Kamalanathsharma and Rakha (*17*)	Optimization	Multi-stage dynamic programming	No	No	No	19%
De Nunzio et al. (*18*)	Optimization	Pruning algorithms / optimal control	No	No	No	10%
Mahler and Vahidi (*19*)	Optimization	Predictive optimal velocity-planning	No	No	Yes	16%
Hao et al. (*14*)	Rule-based	Robust strategy for signal actuation	No	No	Yes	12%
Wu et al. (*20*)	Optimization	Reachable Region Construction	Yes	Yes	No	28%
Jin et al. (*21*)	Optimization	Power-based mixed integer programing	No	No	No	15%
Hao et al. (*11*)	Optimization	Graph model for energy optimization	No	No	No	22%
Lu et al. (*23*)	Optimization	Mixed integer Linear Programming	No	No	No	17%
Hao et al. (*24*)	Optimization	Machine Learning-based Trajectory Planning	No	Yes	No	7%
Altan et al. (*25*)	Rule-based	GlidePath Prototype	No	No	No	17%
Jiang et al. (*26*)	Rule-based	EAD for left-turn vehicles	No	Yes	No	9%
Ye et al. (*27*)	Machine-Learning	Deep learning based queue-aware EAD	No	Yes	No	21%
Guo et al. (*28*)	Optimization	Bi-Level model predictive control	No	No	No	NA
Wan et al. (*29*)	Rule-based	Scenario based speed advisory System	No	Yes	No	16%
Jiang et al. (*30*)	Optimization	Pontryagin's Minimum Principle	No	Yes	No	7%
He et al. (*31*)	Optimization	Multi-stage optimal control	No	Yes	No	41%

queue on the optimal vehicle speed trajectory (*31*). All the above studies were designed for eco-driving at a single intersection, without considering the potential synergy or conflict between EAD strategies for each intersection when approaching multiple connected intersections along a corridor. Therefore, such methods will only reach a sub-optimal energy-saving solution for a corridor case.

When considering various EAD applications, most of the existing studies are designed to apply to internal combustion engine (ICE) vehicles, especially gasoline-powered passenger cars. For example, Hao et al. developed an EAD application traveling through actuated traffic signals. They tested the application in real world, achieving 6% fuel savings when the test vehicle was within the range of communication with traffic signals (*8*). Ye et al. developed a prediction-based EAD model to predict the state of the preceding vehicle for calculating the optimal speed profile for the host vehicle (*7*). Asadi et al. proposed a rule-based control algorithm to schedule an optimum speed trajectory for the vehicle using the short-range radar and traffic signal information (*13*). In recent years, some studies have applied EAD to electric vehicles, which, unlike ICE vehicles, can recoup some energy from braking through regeneration. For instance, Lu et al. used linear programming to calculate the optimal speed trajectory for electric vehicles with consideration of their regenerative braking capability (*23*). Qi et al. designed an EAD system for electric vehicles based on real-world driving data and found that around 15% energy savings can be achieved with the system (*32*). Bai et al. developed a hybrid reinforcement learning-based eco-driving system for electric vehicles to efficiently pass the intersections using both signal timing and surrounding traffic information precepted from sensors (*33*). Some works have studied

the impact of EAD on heavy-duty vehicles. Wang et al. developed a connected EAD system on heavy duty diesel trucks with cellular-based communications and conducted field tests in Carson, California (*34*). Hao et al. developed a truck EAD system based on the SPaT messages and road grade (*11*). Numerical experiments are conducted at a hypothetical pre-timed signalized intersection with varying entry times, speeds, and terrains. Compared to an uninformed driver, the energy savings reached 11.0% for level terrain, 5.8% for uphill terrain, and 20.2% for the downhill case. According to the best knowledge of the author, there is no study that evaluates the potential energy savings of EAD for electric trucks, and there is also limited research on the EAD performance comparison between electric trucks and diesel trucks.

As essential components of EAD application, signal timing and traffic conditions usually appear to be highly dynamic and uncertain in the scope of different road networks. In this dissertation, by analyzing the prior distribution of the queue and SPaT data of the complex scenario, and unique powertrain dynamics of the targeted vehicle type and model, a comprehensive framework of EAD algorithm is proposed for safe, robust, and real-time capable eco-driving strategies.

1.3 Contributions

To optimize the connected eco vehicle trajectory under the uncertain information and make the EAD system applicable for all vehicle types in sequential signalized corridors, this dissertation focuses on analyzing the possible upcoming traffic/signal information, and vehicle dynamics to generate the most energy-efficient solution for the host vehicle while driving in complex traffic scenarios. A large amount of historical data for intersection signal and queue information has been collected and trained using different machine-learning techniques. More specifically, the contributions of this dissertation include:

1) A comprehensive framework for adaptive connected eco-driving strategy under mixed traffic conditions has been designed. By analyzing the possible upcoming traffic and signal information for study intersection or corridor, the designed framework could apply to different types of vehicles without sacrificing safety and mobility.
2) A learning-based model for efficient computation has been proposed. This model is trained on existed/developed optimization methods using collected historical traffic data to guarantee optimality.
3) The traditional EAD algorithm has been extended for corridor-level optimization. By receiving inputs of all the SPaT data from the signal controllers downstream, the algorithm can reach a global minimum of expected energy consumption.
4) Based on the result from simulations, an overall energy saving between 10-20% and 1.4%-6.5% can be achieved by gasoline cars and battery electric trucks under a complex mixed traffic scenario, respectively.

1.4 Organization

The rest of the dissertation is organized as follows. Chapter 2 presents the fundamentals of adaptive eco-driving with some definitions and system framework. Chapter 3 presents an adaptive connected eco-driving strategy to optimize the energy consumption at the intersection considering preceding traffic and possible queues. Chapter 4 describes an adaptive EAD strategy for human drivers or automated vehicle controllers to minimize the expected energy consumption when passing an actuated signalized intersection. Chapter 5 extends the intersection-based eco-driving strategy to actuated signalized corridors, to take care of the uncertain dynamic nature of corridor-wise actuated signal control system. In Chapter 6, a connected EAD algorithm designed specifically for battery electric trucks is designed and tested in complex eco-driving scenarios with multiple connected and non-connected traffic signals. Finally, Chapter 7 concludes the dissertation and provides directions for future work.

2. Fundamentals in Connected Eco-Driving

In this chapter, we introduce the proposed connected eco-driving framework that could accommodate the host vehicle, traffic and signal timing information. Fundamental concepts, including variables, definitions and assumptions, are presented in this chapter to better support the mathematical modeling for this dissertation.

2.1 Problem Statement

In the proposed adaptive connected eco-driving system, ten types of information are fed into the algorithms to derive the most energy-efficient solution for the equipped vehicle. Their definitions are as follows:

1. Distance to intersection (D): the road distance from the current GPS location to the stop line.

2. Vehicle speed (V): the current speed of the vehicle, measured by on-board diagnostics (OBD) devices or GPS devices.

3. Time (t): current time stamp.

4. V2I communication range (C): this application works for both Dedicated Short-Range Communications (DSRC) or C-V2X. The V2I communication range is usually limited by the technology. As the connected eco-driving application start to work when the vehicle is within the communication range, we can assume $D \leq C$.

5. SPaT information: when a CV approaches within V2I communication range, it could receive SPaT information. Depending on whether the signal is fixed timing or actuated,

one would know the phase status and the real/expected start and end time of the current phase.

6. Onboard sensor range (S): The maximum reliable forward detection range of the onboard sensor (e.g. radar, lidar or camera). Usually this range is less than the V2I communication range C, i.e. $S<C$.

7. Distance to the preceding vehicle (R): The measured distance to the preceding vehicle at the same lane. If there is no vehicle detected within the sensor range S, R = -1.

8. Speed of the preceding vehicle (U): The speed of the preceding vehicle at the same lane. If there is no vehicle detected within the sensor range S, U = -1.

9. The vehicle powertrain: The unique energy consumption model of the vehicle related to its speed and acceleration.

10. The prior distribution of the queue length Q (in vehicle number), summarized from the historical traffic data. The prior probability of $P(Q=q)$ is a pre-defined function $f(q)$. The cumulative probability, $P(Q\leq q)$, is defined as $F(q)$.

We assume the sensors only report the states of the adjacent preceding vehicle (if any). Based on the information from sensors, there are three circumstances: 1. No preceding vehicle within the sensor range; 2. A stop preceding vehicle detected; and 3. A moving preceding vehicle detected. Based on the range that the sensor can reach and the distance to the intersection, the following cases are considered when we estimate the queue length or queue length distribution:

Case 1.1. No preceding vehicle is within the sensor range (U = -1) and the vehicle is close to the intersection ($D \leq S$): the queue length is 0.

Case 1.2. No preceding vehicle is within the sensor range (U = -1) and the vehicle is far from the intersection ($D > S$): the possible queue length can vary from 0 to D-S. The conditional probability of the queue length can be formulated as:

$$P(Q = q | U = -1, D > S) = \frac{f(q)}{F(g(D-S))} \tag{2.1}$$

Here we use a function g to convert the queue length in distance into queue length in vehicle number:

$$g(y) = \left\lfloor \frac{y - l_{veh}}{l_{jam}} \right\rfloor + 1 \tag{2.2}$$

where l_{veh} is the average length of vehicle, l_{jam} is the average jam spacing (measured from vehicle font to vehicle front). We select the integer part of the value.

Case 2.1. A stop preceding vehicle is detected (U = 0) and the vehicle is close to the intersection ($D < R$): the preceding vehicle should be a queued vehicle at the downstream intersection if two intersections are closely spaced. In this case, the queue length for the study intersection is 0.

Case 2.2. A stop preceding vehicle is detected (U = 0) and the vehicle is far to the intersection ($D \geq R$): the queue length in distance can be determined as D-R. The queue length in vehicle number is then calculated as $\frac{D-R-l_{veh}}{l_{jam}} + 1$.

Case 3.1. A moving preceding vehicle is detected ($U > 0$) and the vehicle is close to the intersection ($D \leq R$): the preceding vehicle is traveling downstream of the stop line. In this case, the queue length is 0.

Case 3.2. A moving preceding vehicle is detected ($U > 0$) and the vehicle is far from the intersection ($D > R$): the possible queue length in distance can vary from 0 to D-R. The conditional probability of the Q can be formulated as:

$$P(Q = q | U > 0, D > R) = \frac{f(q)}{F(g(D-R))} \quad (2.3)$$

The above cases can be categorized into three types: A. No-queue cases (Case 1.1, 2.1, and 3.1); B. Deterministic queue cases (Case 2.2); and C. Non-deterministic cases (Case 1.2 and 3.2). And we can consider Type A and B as known traffic conditions, and C as unknown traffic conditions.

2.2 Basic Eco-Approach and Departure Model

The most basic scenarios for eco-approach and departure applications will be driving under fixed timing signals without queue. In Hao et al (*8*), a graph-based trajectory planning algorithm was developed to solve the optimal solution for eco-approach and departure. In that paper, we assign a unique 3-D coordinate (t, D, V) to describe the dynamic state of the vehicle, which corresponds to the nodes in the graph. The edges in the graph represent the movement of the vehicle, i.e. state transition from one-time step to the next. The cost on edge as the energy consumption during this state transition process. To formulate this graph model, we discretize the time and space into fixed time step Δt and distance grid Δd. The vehicle speed domain is therefore discretized with $\frac{\Delta x}{\Delta t}$ as the step. The energy consumption

minimization problem is converted into a problem to find the shortest path from the source node *Vs* (*t, D, V*) to the destination node *Vd* (*T, 0, V'*) in the directed graph, where *t, D* and *V* are the current time, distance and speed of the vehicle. *T* is the target passage time at the stop line. For the red time arrival scenario, *T* can be identified as the start of the green time plus a buffer time, i.e. $T = T_g + \tau_b$. *V'* is the target speed when the vehicle passes the stop line. The Dijkstra's algorithm is then applied to solve this single-source shortest path problem. This method shows good performance in energy efficiency but takes relatively long computational time to create the graph and solve it.

In this chapter, to achieve higher computational efficiency and better compatibility with stochastic models, we reformulate this problem into a dynamic programming approach. The objective of this problem is defined as follows:

Give any initial state (*t, D, V*), find the optimal valid action that minimize the expected total cost over the rest of the path to the target state (*T, 0, V'*).

Here we say the transition from State 1 and State 2 is a "valid" action if they satisfy:

1) Time at State 2 is consecutive with time at State 1: $t_2 = t_1 + \Delta t$;

2) Consistency in distance and speed: $D_2 = D_1 + V_1 \Delta t$

3) Speed constraint: $V_2 = V_1 + x\Delta t$ and $V_{min} \leq V_2 \leq V_{max}$, where V_{min} and V_{max} are the minimum and maximum speed allowed.

4) Acceleration constraint: $V_2 = V_1 + x_1 \Delta t$, $(a_{min} \leq x_1 \leq a_{max})$, where a_{min} and a_{max} are the maximum deceleration rate and maximum acceleration rate.

Then we say State 1 is the valid parent state of State 2, and State 2 is the valid child state of State 1. Based on the criteria above, given state (*t, D, V*), the valid actions are included in the set of

$$\{t + \Delta t, D - V\Delta t, V + x\Delta t\}$$

$$a_{min} \le x \le a_{max} \text{ and } V_{min} \le V + x \le V_{max} \tag{2.4}$$

The acceleration rate *x* is therefore the key variable to define a valid action. According to the powertrain model in (*11*) and (*35*), the acceleration is also important in energy estimation for any type of vehicle or powertrain. We can formulate a powertrain-specific function $H(V, x, \Delta t)$ to represent the cost that the study vehicle varies its speed from *V* to $V + x\Delta t$ in Δt time.

We then use $M(t, D, V)$ to represent the minimum total cost at state (*t*, *D*, *V*), which corresponds to a series of optimal valid action from the initial state to the final state. This problem is then formulated in an iterative way as follows:

$$\begin{aligned} M(t, D, V) &= \min_{x} \big(H(V, x, \Delta t) + M(D - V\Delta t, V + x\Delta t, t + \Delta t)\big) \\ s.t.\ & a_{min} \le x \le a_{max} \\ & V_{min} \le V + x \le V_{max} \end{aligned} \tag{2.5}$$

We also define the values of the boundary states at or beyond the stop line. If the vehicle arrives at the stop line at the target time with target speed, $M(T, 0, V') = 0$. For other cases, e.g. 1) if the vehicle exceeds the stop line ($d < 0$); 2) if the vehicle arrives at the stop line at other time ($d = 0, t \neq T$); or 3) the vehicle arrives at the stop line with other speed ($d = 0, V \neq V'$), the total cost function is set to infinity, i.e. $M(t, D, V) = +\infty$.

Based on all the assumptions above, this problem is formulated into a multiple-source single-destination shortest path problem. It can be solved using a variation Dijkstra algorithm in which two nodes are linked only if their time sates are consecutive. The pseudo codes below describe the algorithm. Here we use $X(t, D, V)$ to record the optimal acceleration rate at state (t, D, V).

Initialize the M values of all states with $+\infty$, i.e. $M(t, D, V) = +\infty, X(t, D, V) = 0, \forall t, D, V$.

Set $M(T, 0, V') = 0$.

For $t = T: -\Delta t: T_{min} + \Delta t$

  For each (t, D, V)

    Find all the valid parent states of (t, D, V), i.e. $(t - \Delta t, D + V\Delta t - x\Delta t, V - x), \forall x$

      For each valid action *x*

        If $M(t, D, V) + H(V - x, x, \Delta t) < M(\tau - \Delta t, D + V\Delta t - x\Delta t, V - x)$

          Update $M(t - \Delta t, D + V\Delta t - x\Delta t, V - x) = M(t, D, V) + H(V - x, x, \Delta t)$

          Update $X(t - \Delta t, D + V\Delta t - x\Delta t, V - x) = x$

Return $M(t, D, V)$ and $x(t, D, V)$

Figure 2.1 illustrates a simple example of this algorithm. We use blue, green and red dots to show the states in three consecutive time stamps. Figure 2.1(a) shows the process to find all the valid parent states of each state, using two red states and one green states as examples. Figure 2.1(b) shows that if one state has two or more valid child states, the optimal valid action corresponds to the one with lower M value. Figure 2.1(c) illustrates all the optimal valid actions for the blue and green states based on the proposed algorithm.

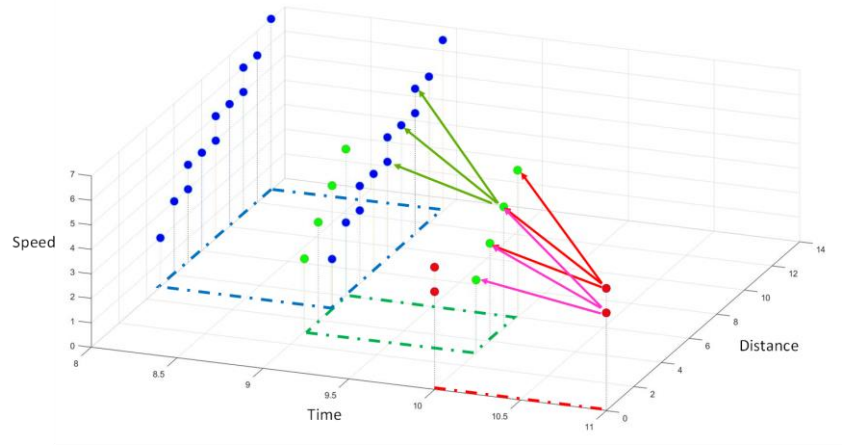

(a) The process to find all the valid parent states

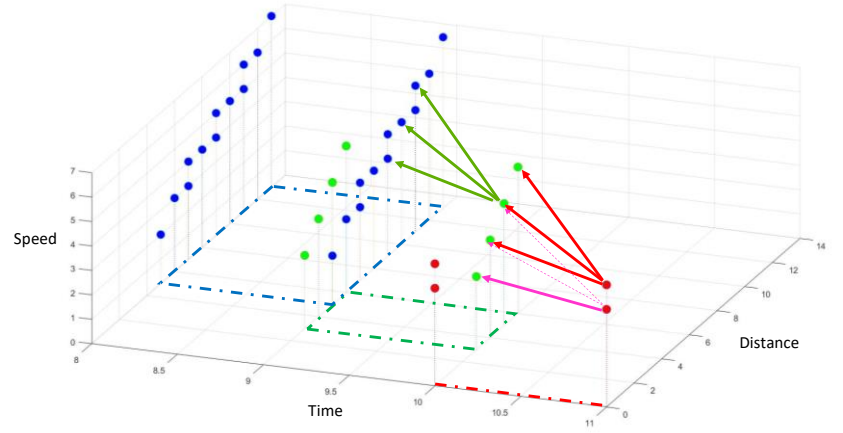

(b) The process to identify the optimal valid actions

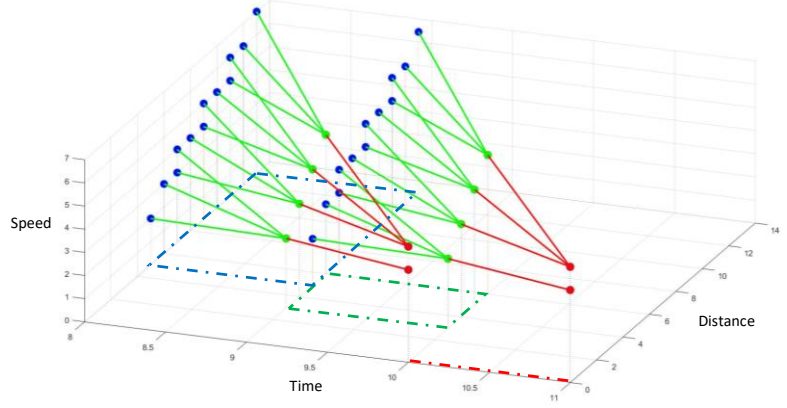

(c) All the optimal valid actions

Figure 2.1 A graph-based illustration of the proposed algorithm

2.3 System Framework

As shown in Figure 2.2, by considering different combinations of input data, signal, traffic, and road networks, a variety of connected eco-driving algorithms are developed to adapt to the dynamic and uncertain traffic and signal conditions. For example, when we have infrastructure data, traffic data, and perception data applied in an environment with fixed timing signal, mixed traffic, and intersection-based network, we can develop an application for EAD under uncertain traffic. If we add the unique powertrain of battery electric trucks (BET) to the previous framework, EAD for BET is proposed. If infrastructure data and perception data are applied in an environment with actuated signal and corridor-based network, application for EAD along actuated signalized corridors is developed. The perception data from the input is to decide whether it's safe to start eco-driving, as well as detecting the position and speed of front vehicles. These algorithms are tested in simulation environments such as VISSIM or MATLAB and evaluated using Motor Vehicle Emission Simulator (MOVES) model. More specifically, the main EAD applications of this dissertation include:

1) Design an adaptive connected eco-driving strategy to optimize the energy consumption at the intersection considering preceding traffic and queues, using radar detection, historical traffic, and SPaT data. This system solves the problem when eco-driving starts too late due to the limitation of the communication and sensing range. Compared to the basic EAD algorithm in Chapter 2.2, this application requires additional queue distribution as input. Numerical simulations have shown that the proposed method is robust and adaptive to varying traffic and queue conditions, and could achieve around 9% energy savings compared to other baseline methods.

2) Develop an adaptive EAD strategy for human drivers or automated vehicle controllers to minimize the expected energy consumption when passing an actuated signalized intersection. A dynamic programming approach is applied to identify the optimal speed for each vehicle-signal state iteratively from downstream to upstream. Additionally, historical SPaT data are used as input for the system. Real-world SPaT data collected from the intersection of Wilmington Avenue and E Carson Street in Carson, CA is applied in the simulation, which has shown that the proposed method is robust and adaptive to varying traffic conditions, and achieves 40% energy savings when the vehicle arrives in the red time and 8.5% energy savings when the vehicle arrives in the green time compared to other baseline methods.

3) Extend the eco-driving strategy to actuated signalized corridors to take care of the uncertain dynamic nature of corridor-wise actuated signal control system. A stochastic SPaT model is proposed using historical data to describe this kind of uncertainty, and then an adaptive EAD strategy is developed for vehicles driving at actuated signalized corridors, which can achieve the corridor-wise minimum expected energy. Compared to the previous application, the corridor EAD accepts input of all the SPaT data from the signal controllers in the downstream. This technique is validated using real-world signal data collected from the Innovation Corridor in the city of Riverside, CA and tested in a simulation environment, and achieved an energy savings of 8.8% - 11.8% compared to baseline and 4.4% - 6.2% compared to intersection-based EAD algorithm for the study actuated signal corridor.

4) Lastly, integrate other vehicle powertrain dynamics, such as battery electric trucks

(BETs), into connected eco-driving and conducts simulation tests in complex eco-driving scenarios with multiple connected and non-connected traffic signals. This eco-approach and departure (EAD) algorithm designed for BETs can help these trucks approach and depart signalized intersections in an energy-efficient manner. The proposed algorithm is evaluated in a microscopic traffic simulation network of urban freight corridors in Southern California with multiple connected and non-connected traffic signals. And the simulation results show that the proposed EAD algorithm for BETs could help the host vehicle achieve an energy savings of 1.4% to 6.5% while maintaining a similar travel time under different simulation environments.

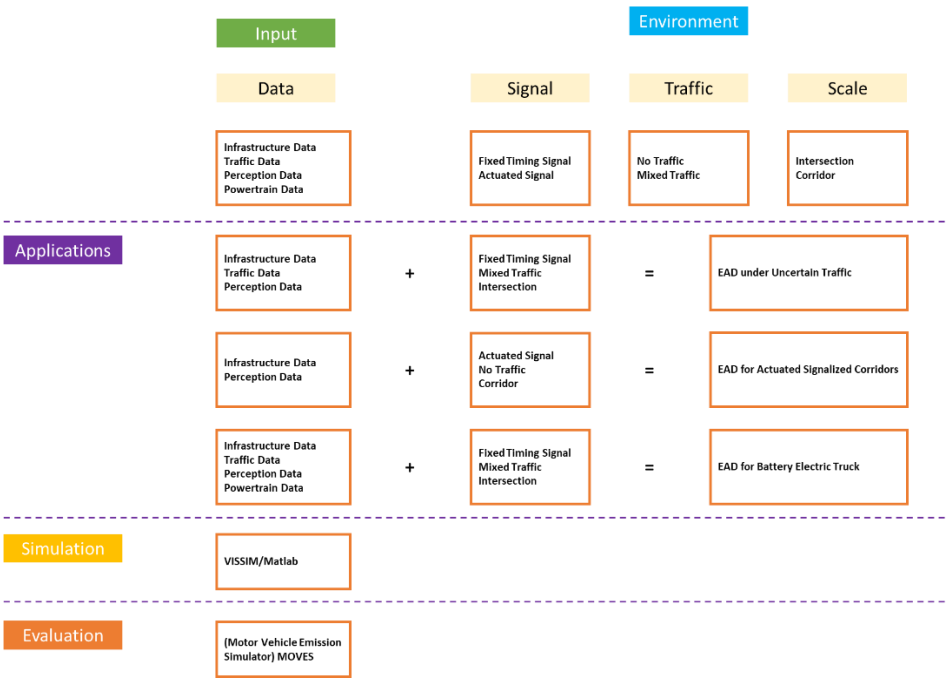

Figure 2.2. EAD applications adapted to different signals, traffic, and road networks.

3. Developing an Adaptive Strategy for Connected Eco-Driving under Uncertain Traffic

In this chapter, we propose an adaptive EAD strategy for vehicles under uncertain traffic conditions, where the host vehicle is far away from the intersection and the exact traffic information, such as the existence of the queue and the length of the queue, couldn't be detected due to the limited sensing and communication range. This algorithm is designed to enable the vehicle to start efficient eco-driving before the detection of queue. A two-phase iterative approach is developed with the use of historical queue distribution. A graph-based model is created with nodes representing states of the host vehicle and traffic conditions, and directed edges with weight representing expected energy consumption between two connected states. The shortest path is calculated that minimizes the total energy consumption for vehicles approaching a pre-timed signalized intersection. Numerical simulations have shown that the proposed method is robust and adaptive to varying traffic and queue conditions, and could achieve around 9% energy savings compared to other methods.

3.1 Introduction

Early EAD studies usually made no-preceding traffic or fixed-timing signal assumptions to avoid the uncertainty in the traffic condition (*8-9, 12*). Some research applied deterministic models to consider the impact of preceding queues to the EAD process. He et al. obtained the speed profile by solving a multi-stage optimal function and put the queue information into constraints (*31*), Ye et al. estimated the end of the queue based on the

predicted preceding vehicle trajectories, with an assumption under congested urban traffic scenario such that a preceding vehicle could always be detected after SPaT messages are received (*22*). All the above studies were conducted under the assumption that either queue does not exist or is fully predictable before trajectory planning. If the radar does not have enough sensing range to detect the preceding vehicle after signal information is received, those studies will not be able or will be less effective to design an optimal speed profile for drivers or longitudinal controller to follow.

In this work, we propose a two-phase iterative approach to adapt the uncertain queue information, so that the vehicle could start eco-driving once entering the communication range even without knowing the current queue information. The first phase creates the speed profile after detecting the end of the queue based on the information acquired from I2V/V2V communication and onboard sensors (radar). The second phase derives the speed profile starting from the receiving of the SPaT messages to the detection of the end of the queue, through analyzing the signal information and potential traffic condition based on historical data (queue distribution). The most energy-efficient solution can be then derived from minimizing the expectation of the energy consumption of all possible actions after combining the two phases.

3.2 Problem Formulation

When a CV approaches within the communication range of a signalized intersection, it could receive SPaT information and know the status of the current traffic signal with the starting and remaining time for the current phase. If the preceding vehicles are within the detection range of the CV equipped radar, the speed and the location of that vehicle could

be measured, and the stop location of the queue could be determined if the measured speed reaches zero. The goal of the method is to design an energy-efficient speed profile while not causing addiotnal delays to the following vehicles. Therefore, the host vehicle should pass the traffic signal right after the nearest preceding vehicle (defined as NPV) in the same lane in an energy-efficient manner.

There are several scenarios that the vehicle might enter if trying to pass the signalized intersection after receiving the SPaT information. If the current signal is green and NPV is detected to be moving, the host vehicle could follow the NPV with an eco-adaptive cruise control strategy. If the current signal is green and NPV is detected to stop, then the estimated time that the vehicle should arrive at the intersection could be calculated from the starting time of the current signal phase with extra reaching time depending on the location of the stop caused by the shockwave theory. If the current signal is red then NPV is most likely to be detected to a stop at some time during the trajectory, and the radar sensing range together with the distance between NPV and host vehicle restricts the distance of eco-driving. For all the cases discussed above, the NPV's stop location is crucial to determine the optimal speed profile for the host vehicle as it affects the location and time when eco-driving could start and finish. However, due to the radar's limited sensing range (most likely smaller then communication range), the host vehicle is usually very close to the queue when the NPV is detected to a stop and it is too late to start eco-driving at that moment. To start the trajectory planning at an earlier stage when SPaT messages are first received, we must deal with the partially observed traffic condition, or the uncertain queue position.

The proposed method divides the process into two parts which are separated by the time that the stop of NPV is detected. The first part involves the uncertainty of the traffic condition and the second part is deterministic with trajectory always reaching an absolute optimal. Therefore, we first construct the graph of the second part of the process and name it as Phase I, and then the graph of the first part of the process can be derived based on the original graph, which is named as Phase II. In the graph, the nodes represent different states of the vehicle and traffic condition, and directed edges with weight representing expected energy consumption between two connected states. A state points to four properties, which are distance to traffic signal (D), passing time after SPaT is first received (t), speed (V) and number of cars queuing by the traffic signal (Q). Two nodes can be connected if the vehicle can reach from one state to another in the minimum time interval (Δt). And for a certain state, as long as the predefined final state is reachable, the next state the vehicle visits in the best solution path is always stable. For example, for a state with parameter [$D = D_1$, $t = t_1$, $V = v_1$, $Q = Q_1$], the next state it could visit has parameter [$D = D_1 - V_1 \times \Delta t$, $t = t_1 + \Delta t$, $V = V_2$, $Q = Q_1$] and v_2 should be deterministic if the state is in the best solution path. Then we iterate over all possible states to guarantee the minimum energy path chosen correctly.

As aforementioned, the proposed iterative method can be divided into two phases. In the first phase, we want to derive an optimal speed profile for the trajectory under the condition of known queue. This includes the position of host vehicle from the point that queue can be first detected by the radar until the vehicle reaches the traffic light ($0 \leq D \leq S + max(L_{Queue})$, where S is the sensing range of radar and L_{Queue} is the queue length by the traffic signal depending on the length per vehicle and number of vehicles). In the second

phase, we want to derive the trajectory speed profile under the condition of unknown queue. This includes the position from the point that SPaT information is first received until the latest point that queue can be first detected ($min(L_{Queue}) + S \leq D \leq C$, where C is the communication range of DSRC). Figure 3.1 shows a sample trajectory of the two phases for a vehicle approaching the traffic signal where there is a queue waiting by. Implementation details of the two phases are given in subsections 2.3.1 and 2.3.2.

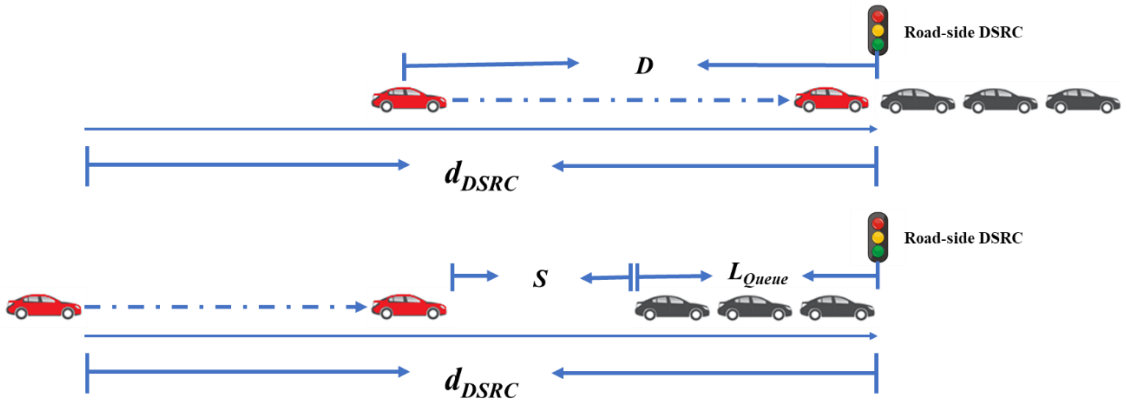

Figure 3.1. Sample trajectory of a host CAV (red) approaching the traffic signal in two phases

3.3 Two-Phase Graph-based Optimization

3.3.1 Phase I Optimization

In Phase I, the end of queue is fully detected for trajectory planning. First, we define all possible states in the vehicle trajectory and initialize a state-energy matrix $M(t, D, V, Q)$ to represent the minimum total cost at state (t, D, V, Q), which corresponds to a series of optimal valid action from the initial state to the final state. For the cases when queue is not detected, or non-deterministic cases, we define the queue state Q as -1. We can formulate the objective function as below in the optimization problem.

$$\begin{aligned} & M(t,D,V,Q) = \min_{x}\big(H(V,x,\Delta t) + M(D - V\Delta t, V + x\Delta t, t + \Delta t, Q)\big) \\ s.t.\ & a_{min} \le x \le a_{max} \\ & V_{min} \le V + x \le V_{max} \end{aligned} \tag{3.1}$$

where $H(V,x,\Delta t)$ is a powertrain-specific function to represent the cost that the study vehicle varies its speed from V to $V + x\Delta t$ in Δt time. For certain queue length Q, if the vehicle arrives at the stop line at the corresponding queue-aware target time with target speed, $M(T(Q),0,V',Q) = 0$. For other cases, the M values are set to infinity.

The pseudocode for Phase I is shown as below:

Initialize the M values of all states with $+\infty$, i.e. $M(t,D,V,Q) = +\infty, X(t,D,V,Q) = 0, \forall t,D,V,Q$.

Set $M(T,0,V',Q) = 0$.

For $t = T: -\Delta t: T_{min} + \Delta t$

  For each (t,D,V,Q)

    Find all the valid parent states of (t,D,V,Q), i.e. $(t - \Delta t, D + V\Delta t - x\Delta t, V - x,\ Q), \forall x$

      For each valid action x

        If $M(t,D,V,Q) + H(V - x,x,\Delta t) < M(\tau - \Delta t, D + V\Delta t - x\Delta t, V - x,\ Q)$

          Update $M(t - \Delta t, D + V\Delta t - x\Delta t, V - x, Q) = M(t,D,V,\ Q) + H(V - x,x,\Delta t)$

          Update $X(t - \Delta t, D + V\Delta t - x\Delta t, V - x,\ Q) = x$

Return $M(t,D,V,\ Q)$ and $x(t,D,V,Q)$

3.3.2 Phase II Optimization

In Phase II, we continue modifying M for the states whose queue hasn't been detected. For the current state (State1) that queue is unknown, at next time step with a given speed, all the state parameters (State2) that vehicle will enter are stable except the queue state is either known (queue detected by radar) or still unknown. At certain non-deterministic state $(t,D,V,-1)$, the conditional probability that the actual queue length q is $\frac{f(q)}{F(g(D-S))}$. We can

define the potential queue pool for the current state as $\{0, 1, 2, \ldots g(D-S)\}$. In the next time step, the vehicle precedes with distance of *V*. There might be two possible scenarios:

Scenario 1. No new detection by next time step. The vehicle is still under non-deterministic state $(D - V\Delta t, V + x\Delta t, t + \Delta t, -1)$, the conditional probabilityof Q=q becomes $\frac{f(q)}{F(g(D-S-V\Delta t))}$. The potential queue pool for becomes $\{0, 1, 2, \ldots g(D-S-V\Delta t)\}$. As $g(D-S-V\Delta t) \leq g(D-S)$, some potential queue lengths are removed from the pool. The prior probability of this scenario, $\mu_{-1} = \frac{F(g(D-S-V\Delta t))}{F(g(D-S))}$.

Scenario 2. The queue is detected by next time step, or the sensing range exceeds the stop line without finding any queue. The vehicle switches to no-queue or deterministic state $(D - V\Delta t, V + x\Delta t, t + \Delta t, Q)$. The queue length q can be any value in the set of $\{g(D-S-V\Delta t)+1, \ldots, g(D-S)\}$. The prior probability of queue length Q=q, $\mu_q = \frac{f(q)}{F(g(D-S))}$.

The objective function is then formulated as follows:

$$\begin{aligned} M(t, D, V, -1) &= \min_x \left(H(V, x, \Delta t) + \mu_{-1}\bar{M}_{-1} + \textstyle\sum_{q=g(D-S-V\Delta t)+1}^{g(D-S)} \mu_q \bar{M}_q \right) \\ s.t.\ & a_{min} \leq x \leq a_{max} \\ & V_{min} \leq V + x \leq V_{max} \end{aligned} \tag{3.2}$$

where $\bar{M}_{-1} = M(D - V\Delta t, V + x\Delta t, t + \Delta t, -1)$, and $\bar{M}_q = M(D - V\Delta t, V + x\Delta t, t + \Delta t, q)$

In equation (3.2), $H(V, x, \Delta t)$ is the immediate cost of the action *x*, $\bar{M}_{-1}$ is the residual cost if the vehicle is still under non-deterministic state by next time step and $\bar{M}_i$ is the residual cost if the queue is detected as Q_i by next time step. The sum of probability μ_{-1} and μ_i's equals to 1. The pseudo-code to solve the problem in (3.2) is shown below.

Initialize M values of all states with $+\infty$, i.e. $M(t,D,V,Q) = +\infty, X(t,D,V,Q) = 0, \forall t,D,V,Q$.

Set $M(T(Q),0,V',Q) = 0$.

For $t = T(Q_{max}): -\Delta t: T_{min} + \Delta t$

For each t, D, V

For $q = 0: 1: Q_{max}$

Find all the valid parent states of (t,D,V,q), i.e. $(t-\Delta t, D+V\Delta t - x\Delta t, V-x, q)$,

and $(t-\Delta t, D+V\Delta t - x\Delta t, V-x, -1), \forall x$

For each valid action *x*

Let $\bar{M}_q = M(t,D,V,q)$, $\mu_q = \frac{f(q)}{F(g(D+V\Delta t - x\Delta t - S))}$

If $M(t,D,V,q) + H(V-x,x,\Delta t) < M(\tau - \Delta t, D+V\Delta t - x\Delta t, V-x, q)$

Update $M(t-\Delta t, D+V\Delta t - x\Delta t, V-x, q) = M(t,D,V,q) + H(V-x,x,\Delta t)$

Update $X(t-\Delta t, D+V\Delta t - x\Delta t, V-x, q) = x$

Find all the valid parent states of $(t,D,V,-1)$, i.e. $(t-\Delta t, D+V\Delta t - x\Delta t, V-x, -1)$

Let $\bar{M}_{-1} = M(t,D,V,-1)$, $\mu_{-1} = \frac{F(g(D-S))}{F(g(D+V\Delta t - x\Delta t - S))}$

For each valid action *x*

If $H(V-x,x,\Delta t) + \sum_{q=-1}^{Q_{max}} \mu_q \bar{M}_q < M(\tau - \Delta t, D+V\Delta t - x\Delta t, V-x, -1)$

Update $M(\tau - \Delta t, D+V\Delta t - x\Delta t, V-x, -1) = H(V-x,x,\Delta t) + \sum_{q=-1}^{Q_{max}} \mu_q \bar{M}_q$

Update $X(t-\Delta t, D+V\Delta t - x\Delta t, V-x, -1) = x$

Return $M(t,D,V,q)$ and $x(t,D,V,q)$

3.4 Simulation Result and Discussion

Simulations are conducted in MATLAB to test the proposed method and compare it with the baseline. Below are the assumptions for all the simulations:

Table 3.1. Simulation assumptions and parameters.

C	Communication range	300 m
$t_{shock\ wave}$	Additional time from shockwave	0 s if Q = 0, else 2(Q+1) s
V_0, V_t	Initial and final speed of the host vehicle	13 m/s
V_{max}	Maximum speed	18 m/s
V_{min}	Minimum speed	0 m/s
a_{max}, - a_{min}	Maximum and minimum acceleration	2 m/s^2
Q	Number of Queueing vehicles	**Z**[0, 20]
Δd_{TL}, Δt, ΔV, ΔQ	minimum interval in the state parameters	1
Vehicle length	length per vehicle	5 m/vehicle

The ideal trajectory for absolute minimum energy consumption can be derived from M when the real queue length is known (i.e. perfect information) at the same time as first SPaT message being received, for example: $d_{Rad} = C$. Besides the ideal method, couple of baseline methods (Baseline_k) are setup for comparison: Assuming the queue length to be Q_k, the vehicle first follows the ideal trajectory of assumed Q_k, length, then change to the corresponding strategy after detecting the real queue length. These baselines are the methods given the same information as the proposed method except the historical queue distribution is missing. Note that if k is 0, Baseline_0 corresponds to the scenario when the vehicle follows the existing EAD strategy with no-queue assumption until the radar detects preceding traffic.

Therefore, all the methods including ideal, proposed and baseline can be evaluated with energy consumption and the result is shown in the following subsections.

3.4.1 Sample Trajectory among Driving Methods

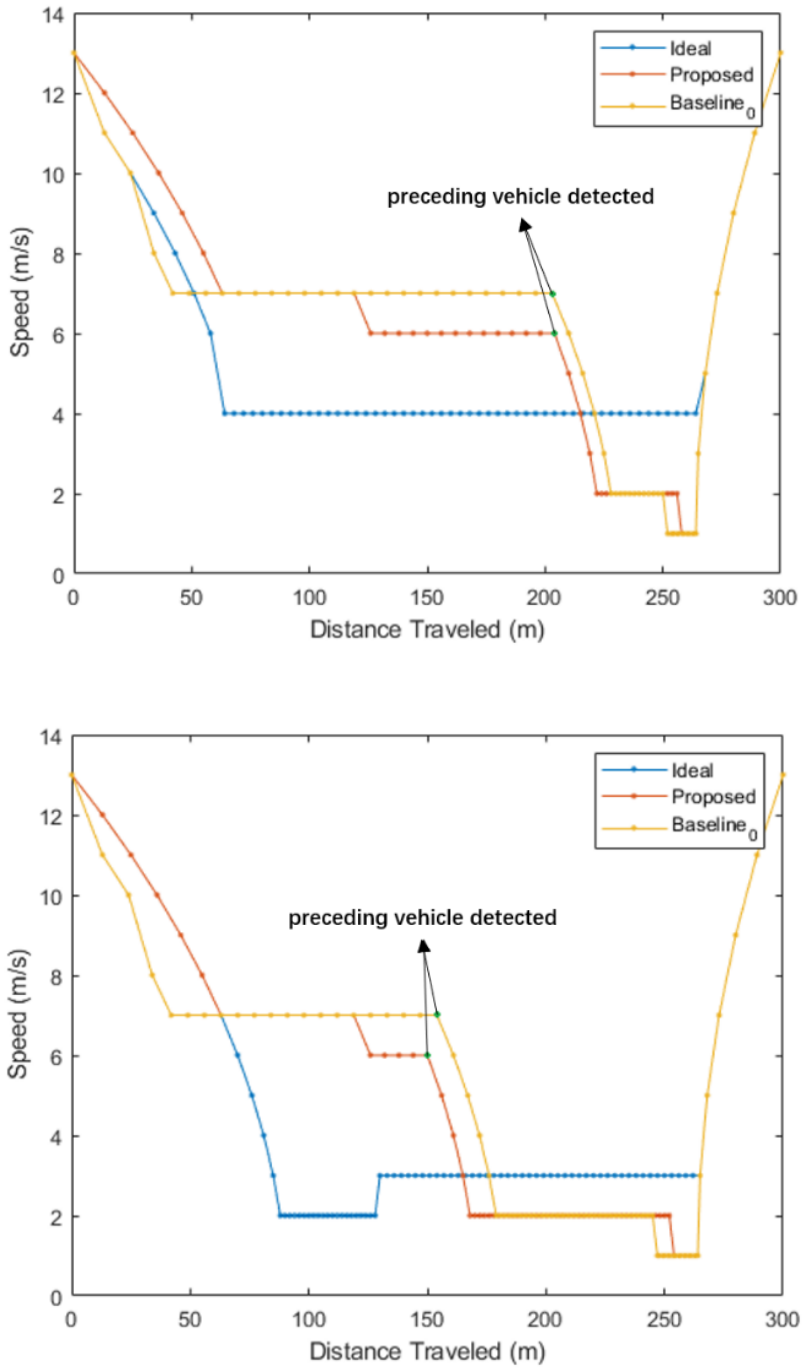

Figure 3.2. Speed profile of proposed against baseline and ideal method with Q = 10 (top) and 20 (bottom).

First, two sample trajectories of the vehicle approaching traffic signal with different queue lengths derived from each method are shown in Figure 3.2. For the baseline method, zero vehicle is assumed to be waiting by the traffic signal and Baseline_0 is used. The other assumptions include: d_{radar} = 50m, t_{SPaT} = 40s and $Q \sim unif\ \{0, 20\}$. As can be seen from the two figures with two queue cases in Figure 3.2, although both proposed method and baseline could react instantly for deceleration when the preceding vehicle is detected, the host vehicle in the proposed method could react 30-70 meters earlier based on the possible queue conditions and prior distributions, resulting in less energy consumption.

3.4.2 Performance Comparison of Energy Consumption

We first compare the energy consumption among different methods for varying exact queue length. All the parameters except real queue length are set as constant values, including:

$$d_{radar} = 100\text{m},\ t_{SPaT} = 40\text{s and } Q \sim unif\ \{0, 20\} \tag{3.3}$$

As shown in Figure 3.3, the proposed method has a lower energy consumption than the baseline methods for most Q and only has a slightly larger energy consumption compared to the ideal method. The baseline_{20} has the largest energy consumption when the real number of queue is 0, due to the huge difference between queue assumption and reality. To compare with all the possible baseline methods, since the Q distribution is uniform, the expected energy consumption (E_{Exp}) is calculated as the average consumption value of all Q, and is shown in Table 3.2. The proposed method reduces the energy consumption by 3.35% (Baseline_0) and 8.88% (average 21 baselines) and is 2.24% higher than the ideal energy consumption.

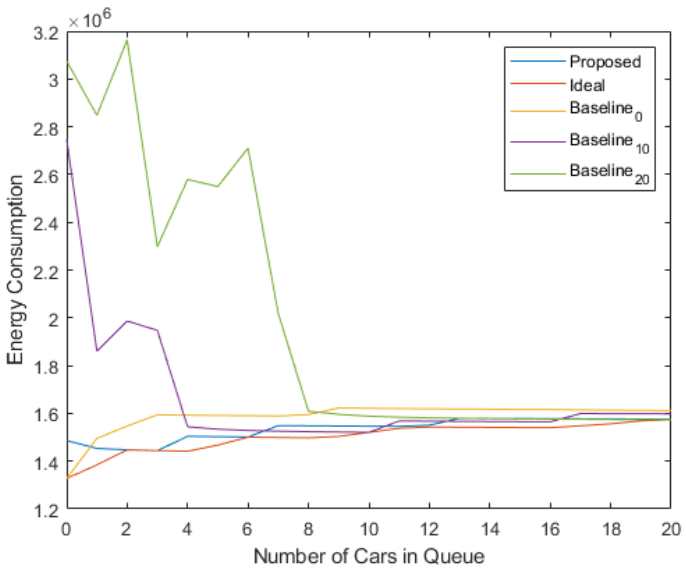

Figure 3.3. Energy comparison (y axis) of proposed against baseline and ideal method in terms of different queue length (x axis)

Table 3.2. Expected energy consumption (E_{Exp})

Method	Energy(10^6)	Method	Energy(10^6)
Ideal	1.5011	$Baseline_{10}$	1.6682
Proposed	**1.5354**	$Baseline_{11}$	1.6998
$Baseline_0$	1.5869	$Baseline_{12}$	1.6235
$Baseline_1$	1.5500	$Baseline_{13}$	1.6506
$Baseline_2$	1.5444	$Baseline_{14}$	1.6727
$Baseline_3$	1.5417	$Baseline_{15}$	1.7176
$Baseline_4$	1.5424	$Baseline_{16}$	1.7365
$Baseline_5$	1.5646	$Baseline_{17}$	1.7949
$Baseline_6$	1.5932	$Baseline_{18}$	1.8532
$Baseline_7$	1.6156	$Baseline_{19}$	1.9315
$Baseline_8$	1.6066	$Baseline_{20}$	1.9908
$Baseline_9$	1.6216		

We then compare the energy consumption among different methods for varying t_{SPaT}, meaning diverse time the vehicle enters the DSRC range and approaches the traffic signal. The same parameters are used except t_{SPaT} (20~60s).

For the ideal method, as shown in Figure 3.4, E_{Exp} is monotonically increasing due to the more frequent acceleration and deceleration during longer travel time. The proposed method shows a better performance than baseline methods when $t_{SPaT} \geq 22$s. The worse performance for small t_{SPaT} is caused by the high acceleration and speed of the vehicle that tries to arrive at the traffic signal at the required time. The energy consumption tends to reach the same value as t_{SPaT} increases among all methods.

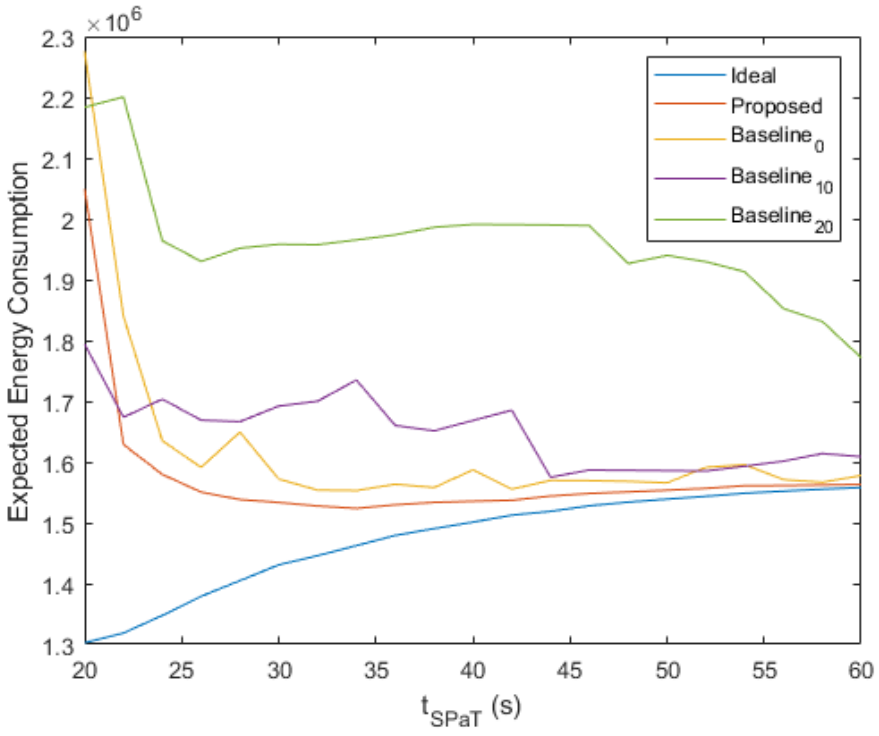

Figure 3.4. E_{Exp} comparison (y axis) of proposed against baseline and ideal method in terms of different t_{SPaT} (x axis)

3.4.3 Comparison of Methods for Varying Radar Range

In this subsection, we want to compare the energy consumption among different methods for varying d_{Rad}. This simulates the various sensing range of all kinds of radars or when

there is a preceding vehicle stopping in front of the host vehicle. The same parameters are used as (5) except d_{Rad} (50~200m).

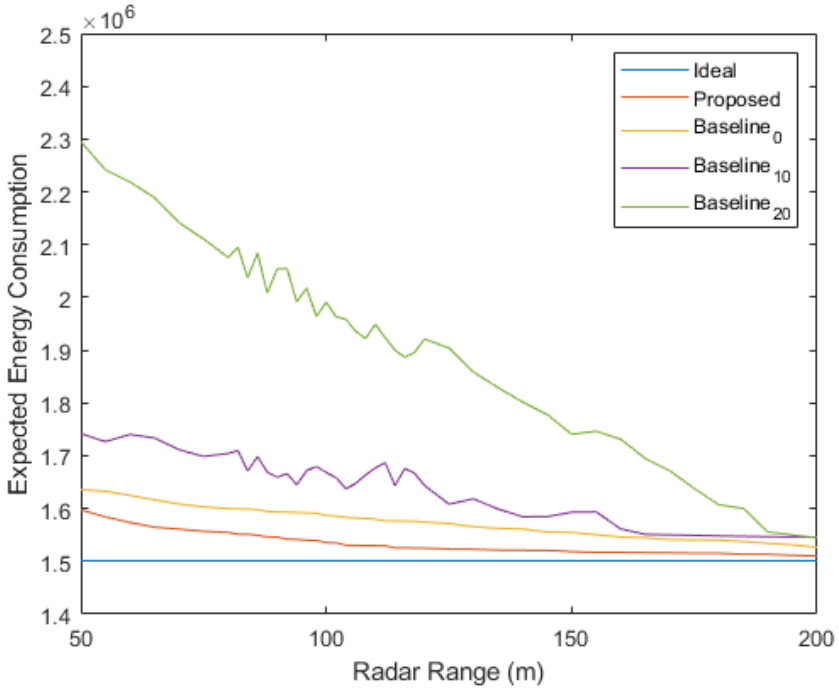

Figure 3.5. E_{Exp} comparison (y axis) of proposed against baseline and ideal method in terms of different radar range (x axis).

As we can see from Figure 3.5, the proposed method always outperforms the baseline method. E_{Exp} of ideal method stays the same for all radar range since the queue length is set to be known from the beginning. For both baseline methods and proposed method, E_{Exp} gradually decreases as d_{Rad} increases, since the distance that queue is known gets longer and a larger portion of the trajectory can result in absolute minimum energy consumption. A detailed E_{Exp} table is shown in Table 3.3. The proposed method consumes less energy for every d_{Rad} compared to the baselines.

Table 3.3. E_{Exp} (10^6) comparison between proposed, baseline and ideal method for different d_{Rad}.

Method / d_{Rad}	Ideal	**Proposed**	Baseline$_0$	Baseline$_{10}$	Baseline$_{20}$
50	1.5011	**1.5973**	1.6360	1.7419	2.2949
60	1.5011	**1.5735**	1.6249	1.7403	2.2186
70	1.5011	**1.5610**	1.6085	1.7115	2.1418
80	1.5011	**1.5549**	1.5998	1.7043	2.0755
90	1.5011	**1.5461**	1.5933	1.6593	2.0540
100	1.5011	**1.5354**	1.5869	1.6682	1.9908
110	1.5011	**1.5297**	1.5797	1.6770	1.9489
120	1.5011	**1.5250**	1.5744	1.6438	1.9214
130	1.5011	**1.5228**	1.5655	1.6184	1.8585
140	1.5011	**1.5209**	1.5612	1.5846	1.8018
150	1.5011	**1.5183**	1.5547	1.5930	1.7407
160	1.5011	**1.5170**	1.5460	1.5614	1.7313
170	1.5011	**1.5161**	1.5411	1.5502	1.6715
180	1.5011	**1.5154**	1.5402	1.5482	1.6071
190	1.5011	**1.5133**	1.5340	1.5466	1.5554
200	1.5011	**1.5103**	1.5265	1.5458	1.5446

3.4.4 Comparison of Methods for Varying Queue Distribution

In this subsection, we want to verify the capability of the proposed method for a different queue distribution. We set $Q \sim N(10, 4)$ with other parameters the same as (5). Table 3.4 shows the comparison of expected energy consumption among different methods. The proposed method reduces the energy consumption by 4.14% (Baseline$_0$) and 3.56% (average 21 baselines) and is 1.88% higher than the ideal consumption.

Table 3.4. E_{Exp} comparison among proposed, baseline and ideal method for Gaussian queue distribution.

Method	Energy(10^6)	Method	Energy(10^6)
Ideal	1.5141	$Baseline_{10}$	1.5693
Proposed	**1.5431**	$Baseline_{11}$	1.5887
$Baseline_0$	1.6070	$Baseline_{12}$	1.5491
$Baseline_1$	1.5695	$Baseline_{13}$	1.5617
$Baseline_2$	1.5624	$Baseline_{14}$	1.5765
$Baseline_3$	1.5552	$Baseline_{15}$	1.5931
$Baseline_4$	1.5433	$Baseline_{16}$	1.6028
$Baseline_5$	1.5604	$Baseline_{17}$	1.6476
$Baseline_6$	1.5619	$Baseline_{18}$	1.6893
$Baseline_7$	1.5487	$Baseline_{19}$	1.7634
$Baseline_8$	1.5444	$Baseline_{20}$	1.8183
$Baseline_9$	1.5479		

3.5 Summary and Discussion

This chapter proposes an adaptive strategy for connected eco-driving towards a pre-timed signalized intersection under uncertain traffic condition. The validation results indicate that the proposed 2-phase iterative approach can achieve an energy-efficient trajectory, given the information of SPaT and historical queue distribution. Numerical simulation results show that the proposed method can save an average of 8.88% energy consumption for uniform queue distribution and 3.56% for Gaussian queue distribution compared to baseline methods. The proposed method also works for varying radar range and different time the vehicle initially enters the DSRC range.

4. Developing an Adaptive Connected Eco-Driving Strategy for Actuated Signals

Most existing EAD applications were developed using rule-based methods which didn't guarantee energy optimality. In this chapter, we developed an adaptive EAD strategy for human drivers or automated vehicle controllers to minimize the expected energy consumption when passing an actuated signalized intersection. The historical signal phase and timing (SPaT) data are applied to calculate the probability that one signal state (including phase status, time in the phase, minimum and maximum time-to-change) transfers to another state. A dynamic programming approach is applied to identify the optimal speed for each vehicle-signal state iteratively from downstream to the upstream. Real-world SPaT data collected from the intersection of Wilmington Avenue and E Carson Street in Carson, CA is applied in the simulation, which has shown that the proposed method is robust and adaptive to varying traffic conditions, and achieves 40% energy savings when the vehicle arrives in the red time and 8.5% energy savings when the vehicle arrives in the green time compared to other baseline methods.

4.1 Introduction

In real-world traffic in the U.S., about 70% of the intersections are controlled by actuated signals. Signal timing usually appears to be dynamic and uncertain due to the high uncertainty in phase extension and skipping caused by vehicle actuation. For example, when a CV is approaching an actuated signalized intersection, the remaining time of the current signal phase indicated by the SPaT message will be updated dynamically due to the

traffic from all directions. For any signal phase of an actuated signal system, the cycle length and phase duration are no longer a constant value. Some researchers will consider using the average phase time to calculate a rough passing window. In Stevanovic et al. (*57*), a rule based green light optimized speed advisory (GLOSA) system was developed for actuated signals and an average green phase time was used to calculate desired speed. Some researchers will consider the green light phase time within a probability distribution. Saldivar-Carranza et al. (*58*) created three different rule-based advice approaches (conservative, balanced, and aggressive) based on the different green phase probability threshold. Some researchers will utilize the minimum and maximum remaining time of the phase broadcasted by the signal controller to provide a rough predictive range in SPaT. In Hao et al. (*8*), a rule-based eco-driving algorithm has been developed based on the assumption that the min/max values in SPaT messages are reliable enough to represent the real upper and lower bound of the phase remaining time. However, the real SPaT data collected from Carson, CA show that even this assumption does not hold in many cases in the real world. Figure 4.1 shows a SPaT example of the major approach of a real intersection. We compare the minimum and maximum remaining time provided in the first second of the phase, along with the exact phase duration. For the green phase, the exact phase duration is not well bounded by the min and max value, especially for cases when the green time is significantly extended due to minor phase skipping. For the red time, the min and max values provide a wide range for the remaining time, which also brings difficulty in phase duration prediction. These issues increase the difficulty to predict the actual remaining time in a phase using signal phase and timing (SPaT) information.

Furthermore, the traditional rule-based methods will also bring difficulty to reach global optimality for lowest energy consumption. These problems further brings a great challenge to derive an energy-efficient speed profile for vehicles to follow.

In this chapter, we propose a graph-based trajectory planning algorithm that solves the optimal speed trajectory solution for actuated signals using the dynamic programming approach. As the physical meaning of SPaT is not always reliable as shown in Figure 4.1, we construct a directional SPaT graph to calculate the probability of one SPaT state changing to the next based on the historical SPaT data. Then, the most energy-efficient solution can be then derived from minimizing the expectation of the energy consumption from the current state to the final state.

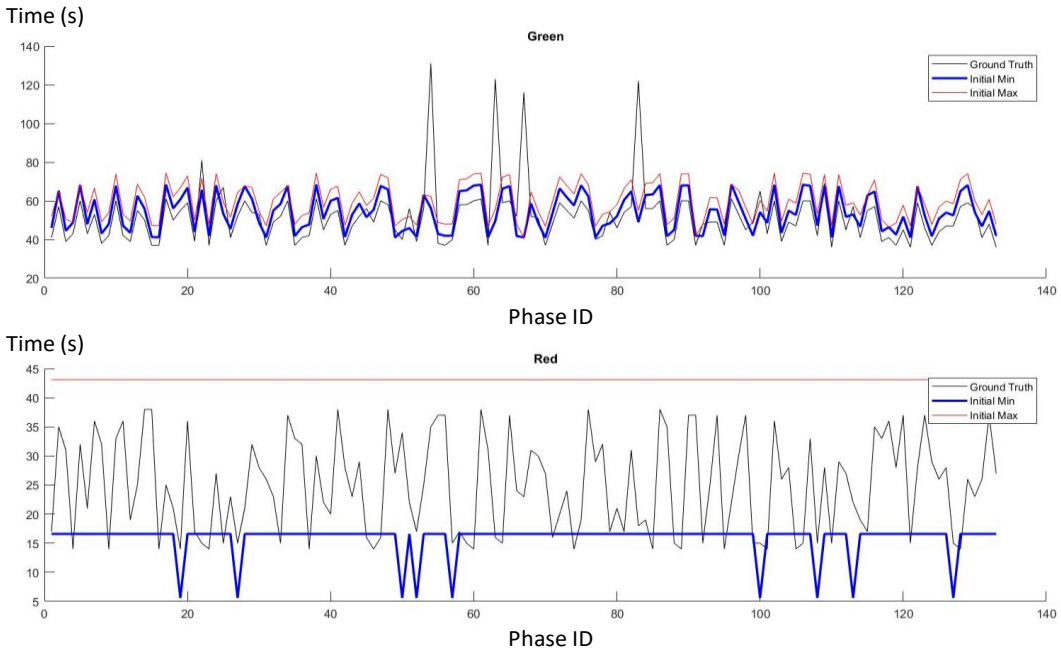

Figure 4.1 Sample SPaT message from a real intersection

4.2 Problem Statement

When a Connected Vehicle approaches an actuated signalized intersection and establishes communication with the signal controller via DSRC or C-V2X, it could receive Signal Phase and Timing (SPaT) message for the current phase. Using the received SPaT information, distance to the traffic signal (D), and the current speed (V), the proposed method can derive the optimal speed profile from the preconstructed energy graph for the minimum expected energy consumption. The host vehicle will then follow the suggested speed to achieve an eco-driving behavior.

There are two major challenges in this problem: 1) how to find the minimum-energy trajectory for eco-driving and 2) how to manage the uncertainty from actuated signals and develop an adaptive strategy. In the next subsection, we will first propose a dynamic programming (DP) based model framework to efficiently investigate the optimal solution for the first challenge. We will then discuss the stochastic SPaT model that can accommodate the model framework, and the adaptive strategy to perform an eco-driving.

4.3 Statistical Model Using Actuated Signal Phase and Timing (SPaT) data

Since the actuated signals make real-time updates according to the dynamic traffic, the SPaT pattern may vary significantly at every cycle for each traffic signal. This uncertainty increases the difficulty of deriving an energy-efficient speed profile. What is worse, there is no official standard to tell which values should be provided as predicted “minimum time-to-change” and “maximum time-to-change” for actuated signals. Are they predicted based on static values from the signal plan sheets, or based on dynamic values considering the real-time vehicle calls? Are they “common” values that represent the typical traffic

situations, or “extreme” values considering emergency vehicle preemption or consecutive phase skipping if there is no traffic on the minor street? Different device manufacturers, traffic operators, and researchers may have different understandings, strategies, and algorithms. Most existing eco-driving methods (*35*) give certain assumptions to the SPaT information from actuated signals. Some of them assume that the minimum time-to-change, maximum time-to-change, or both can converge to the actual time-to-change when the phase comes to an end. However, the real-world SPaT data show that even this assumption does not hold in many cases.

In order to solve the problem of the inaccurate minimum and maximum time-to-change SPaT information for actuated signals, instead of seeing them as time indicators or time-to-pass, we use them purely as parameters to indicate certain states of the traffic signals. And after each time stamp when the SPaT messages are updated, we assume there is a state transition for the actuated signal. We then define the SPaT state W as a set of four parameters: current phase W_P, elapsed time in the current phase(sec) W_T, estimated minimum time to change for the current phase(sec) W_{Min}, and estimated maximum time to change for the current phase(sec) W_{Max}.

Using the data collected from the actuated signal, a directional SPaT graph can be constructed to calculate the probability of one SPaT state changing to the next. The node of the graph represents a specific SPaT state can be represented as $W = (W_P, W_T, W_{Min}, W_{Max})$. A directional edge is connected between two nodes if the current SPaT state has been recorded transitioning between two nodes in the collected data. To help calculate the expected energy reaching the destination from the current state, we use

the probability of this state change to represent the weight of the edge, which can also be estimated from the historical SPaT data. Since the sum of probability transitioning from one certain state to all other states is 1, the sum of weight from one parent node to all its child nodes is also 1, and can be expressed as below:

$$Signal\ state\ graph\ =\ (Vertex, Edge) \tag{4.1}$$

$$\text{with } Vertex = \{W = (W_P, W_T, W_{Min}, W_{Max})\} \text{ for i} = 1 \dots N-1$$

$$Edge = \{(W_i, W_j)\} \text{ for connected } i\text{th and } j\text{th signal state}$$

$$\sum_{\forall j} Weight_{W_i \to W_j} = 1$$

Figure 4.2 shows an example of the proposed directional SPaT graph in the red phase. The numbers in each red node represent the elapsed time in the current phase, estimated minimum total time, estimated maximum total time from top to bottom. For given red state W = {Red, 20,21,40}, the exact remaining time of the red phase can be 1s, 2s, 3s, or more. After the SPaT graph is constructed, the probability of one state changing to the next can be calculated using the weight of the edge divided by the total weight of the outgoing edges.

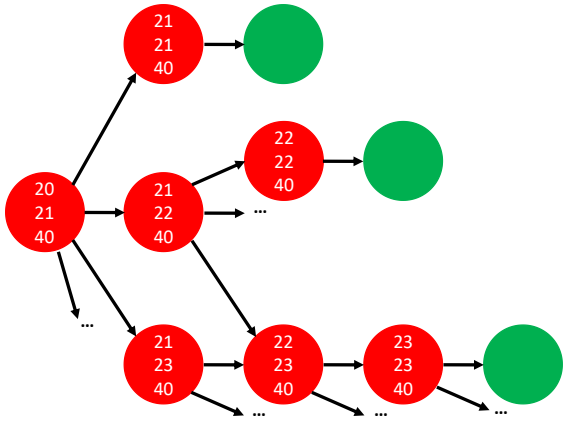

Figure 4.2. Directional SPaT Graph in the Red Phase

The SPaT data applied in the algorithm were collected from the northbound of the intersection between Wilmington Avenue and E Carson Street in Carson, CA. The data were preprocessed so that only the 9 am-12 pm period between Dec 11th, 2018 to May 2nd, 2019 was included. A certain period-of-time enables less plan variation and uncertainty in the graph construction, which makes the suggested speed more accurate for energy saving. All the time parameters are rounded to integers to decrease the number of nodes and reduce the size of the SPaT graph, so that the calculation is fast enough for real-time calculation.

For certain vehicle dynamic state (t, D, V) and SPaT state W = (W_T, W_{min}, W_{max}), the objective function is then formulated as follows:

$$\begin{aligned} M(t,D,V,W) &= \min_{x}\left(H(V,x,\Delta t)+\sum \mu_{W\to W'} M'_{W'}\right) \\ s.t.\ & a_{min}\le x\le a_{max} \\ & V_{min}\le V+x\le V_{max} \end{aligned} \tag{4.2}$$

Where W' is the possible SPaT state in the next time step, $M'_{W'}$ = M{t+Δt, D-VΔt, V+xΔt, W' }is the residual cost if the next SPaT state is W', and $\mu_{W\to W'}$ is the probability that the next SPaT state is W'. The sum of probability $\mu_{W\to W'}$ equals to 1.

As the boundary condition of the model, we defined the start of the green phase after the end of each red phase as the final state for the graph and formulate the remaining trajectory of the vehicle using rules. For a certain final state (T_g, D, V), if the final speed V is less than the target speed V', an acceleration trajectory will be added with the maximum acceleration. If the final speed V is greater than or equal to the target speed V', a constant speed trajectory is added to reach the stop line. The residual cost at this state is the total energy consumption of the added trajectory plus a time penalty, which is a linear function

of the elapsed time count for the time lost and encourage a fast and efficient intersection passing. Similar state definition is created for the green light phase. The yellow phase (y_1) is assumed to have a duration of 3 sec and is created as the first second of the yellow light after the green light phase. For the states containing y_1, if $d_{TL}/v \leq 3$, the vehicle will simply cross the road at its current constant velocity. If $d_{TL}/v > 3$, the vehicle will enter the red phase time before it reaches the intersection, and the graph created for red light is applied for energy-efficient driving. The design of the remaining trajectories and the energy penalty ensure a fair comparison between the proposed algorithm and other baseline methods.

The proposed method applies to any type of vehicle and powertrain if the powertrain-specific function $H(V, x, \Delta t)$ is given. In this work, we use the tractive power of a typical passenger car as the cost function of the proposed graphical model. Further tests with more vehicle types will be conducted in the future.

4.4 Case Study and Results

Simulations are conducted in MATLAB to test the proposed method and compare it with the baseline. The testing is done separately on red and green phases using the SPaT graph created by the collected data. To compare the energy consumption between the proposed and baseline method, a total of 5000 historical SPaT messages are tested with different phase-entering time and initial velocity. Table 4.1 below shows the assumptions for all the simulation parameters in both the red and green light phase.

Table 4.1. Simulation Assumptions and Parameters.

C	Communication range	300 m
v_t	The final speed of the host vehicle at the intersection	13 m/s
v_{max}	Maximum speed	18 m/s
v_{min}	Minimum speed	0 m/s
a_{max}, - a_{min}	Maximum and minimum acceleration	2 m/s^2
Δd_{TL}, Δt, Δv	Discrete interval in the state parameters for distance, time and speed	1

4.4.1 Simulation Results for Red-time Arrival

For the case that the vehicle approaches the intersection in the red time, the baseline driver models are developed as follows: when the host vehicle enters the study zone, the vehicle will first accelerate to the maximum speed using the constant acceleration, then decelerate after reaching the safety distance. The safety distance is defined as the shortest distance the vehicle needs to stop at the intersection with the maximum deceleration. If the traffic signal changes to green phase in this process, the vehicle will accelerate with the maximum acceleration and pass the intersection as soon as possible.

Table 4.2. Simulation results for red-time arrival: proposed, baseline and saving (Unit: 10^6 J)

T_0 (s) / V_0 (m/s)	0			20			40			60		
5	1.75	3.42	49%	1.65	3.44	52%	1.67	3.43	51%	1.87	3.51	47%
9	1.62	3.22	50%	1.61	3.24	50%	1.52	3.21	53%	1.59	3.27	51%
13	1.54	2.38	35%	1.57	2.40	35%	1.47	2.37	38%	1.48	2.43	39%
17	1.45	1.53	5%	1.46	1.56	6%	1.43	1.53	7%	1.44	1.56	8%

As mentioned in the previous section, if the final speed V' between the baseline and proposed method is different, extra energy is added to the one with lower speed to quantify the speed gap as a form of energy to ensure a fair comparison. A similar energy penalty is added to the one with longer travel time for the same reason. Table 4.2 shows the average energy consumption (10^6 J) between two methods (proposed and baseline) over all available SPaT messages with different phase-entering time and initial velocity, along with the energy saving in percentage. The top row T_0 represents the phase-entering time (s) in each run and the column V_0 represents the initial velocity (m/s).

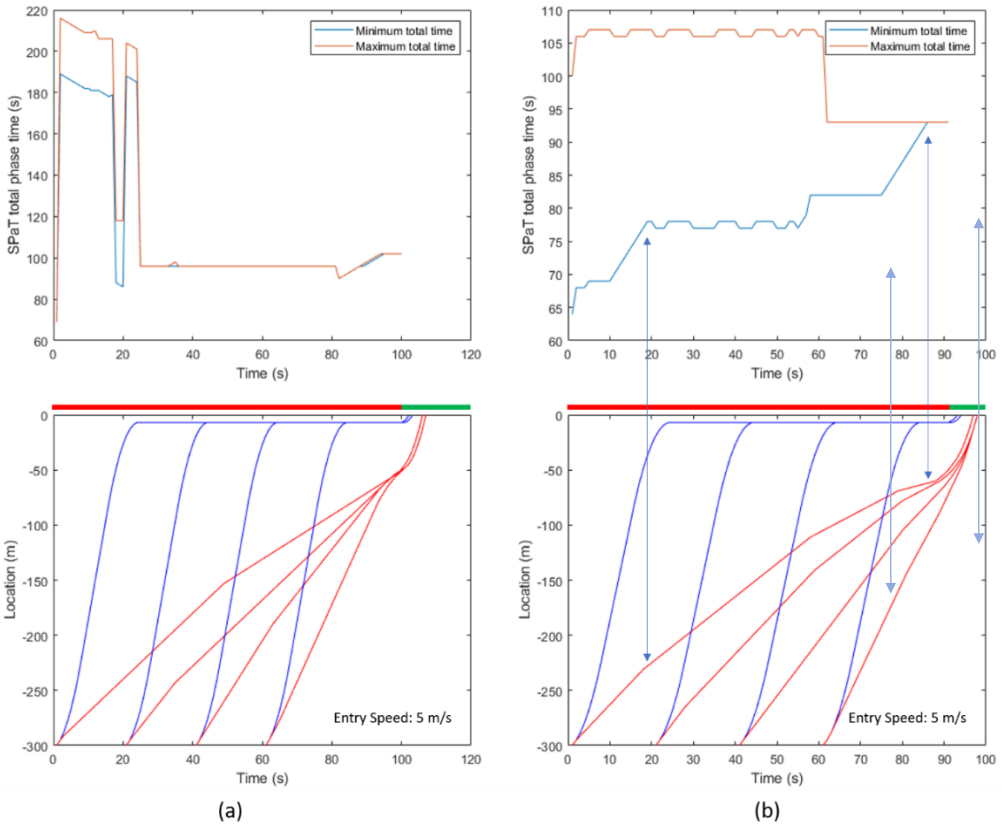

Figure 4.3. SPaT phase time (upper) and sample trajectory (lower) of the baseline vs. proposed algorithm

As can be seen from the table, the energy consumption decreases as the initial velocity increases, due to a higher initial kinetic energy of the host CV. Since the total travel distance is the same, the phase entering time has little impact on the energy when the vehicle has the same initial velocity. The SPaT data and sample speed profiles of the proposed algorithm and the baseline with different phase entering time are shown in Figure 4.3. In the upper images, x-coordinates represent the time in the red phase, and y-coordinates represent the estimated total phase duration. Then two curves are plotted in each image. The red curve represents the minimum phase duration suggested by the SPaT message, and the blue one represents the maximum phase duration. Figure 4.3(a) and (b) show two different types of SPaT conditions. In the case shown in Figure 4.3 (a), minimum and maximum values quickly converge after some initial oscillation. The EAD trajectory (red curve) shown in the lower image looks insensitive to the SPaT update in this case as the remaining time is still long when the update happens. In the case shown in Figure 4.3 (b), minimum and maximum values gradually converge in terms of time. The EAD trajectory entering from time 0s sensitively updates its speed whenever the SPaT updates, On the contrary, the EAD trajectory entering from time 40s or 60s is not responsive to the updates as they are still far from the stop line at those moments. The sample trajectories with the same initial speed and location, but different phase entering time are shown in the lower images. Compared with the baseline trajectories (blue curves in the lower images), the eco-driving trajectory avoids the sharp deceleration and relatively long wait at the intersection. The speed of the host vehicle is optimized corresponding to the received SPaT messages and distance to the intersection, and both the connected and baseline vehicles

arrived at the intersection at roughly the same time. The proposed method always outperforms the baseline method. A 5.23% ~ 52.65% energy saving can be achieved using the proposed method and the average energy saving is over 40%.

4.4.2 Simulation Results for Green-time Arrival

For the case that the vehicle approaches the intersection in the green time, the baseline driver is designed as follows: if the current speed of the vehicle is less than 13m/s, the vehicle will accelerate to 13 m/s using an acceleration of 1 m/s^2 and pass the intersection. If the current speed is higher than 13m/s, the vehicle will decelerate to 13 m/s using an acceleration of -1 m/s^2 and pass the intersection. And the vehicle will keep its current speed if it is driving at 13m/s.

Table 4.3. Simulation results for green-time arrival: proposed, baseline and saving (Unit: 10^6 J)

T_0 (s) / V_0 (m/s)	0			20			40			60		
5	4.47	4.61	3%	4.56	4.66	2%	8.16	8.22	1%	6.27	7.01	11%
9	3.93	3.96	1%	3.97	4.01	1%	7.18	7.72	7%	6.24	6.91	10%
13	3.31	3.31	0%	3.32	3.36	1%	6.97	7.08	2%	6.21	6.26	1%
17	2.68	3.02	11%	2.63	3.1	15%	2.8	6.85	59%	6.25	6.14	-2%

A similar energy-time-velocity transformation is used to quantify the speed gap as a form of energy. Table 4.3 shows the average energy consumption (10^6 J) and saving (%) between two methods over all available SPaT messages with different phase-entering time and initial velocity. The table has the same configuration as Table 4.2.

The same V_0 vs. energy trend occurs as seen in the red phase. Higher energy consumption is seen with larger T_0, since the vehicle has limited time to pass the intersection and the

room for speed optimization is limited. As can be seen from the table, the proposed method outperforms the baselines for most cases except for the 25s phase-entering time at 17m/s initial speed. For the 25s phase-entering time, the remaining green time in the current phase becomes too little for the vehicle to pass. Therefore, a relatively conservative strategy in the baseline turns out to be more energy-efficient. On average, 8.5% of energy savings can be achieved when the vehicle arrives in the green time compared to the baseline method. A much lower saving in the green phase compared to the red phase is because the proposed graph-based algorithm performs similarly to the baseline in many cases, unlike the red phase where host vehicles often need to decelerate or accelerate in advance to accommodate for the passing interval.

4.5 Summary and Discussion

This chapter proposes an adaptive strategy for connected eco-driving towards an actuated signalized intersection. Energy comparison is conducted between the proposed method and the baseline in consideration of different speed and time. The validation results indicate that the proposed DP-based statistical model can achieve an energy-efficient trajectory, given the information of historical SPaT information. Numerical simulation results show that the proposed method can achieve 40% energy savings when the vehicle arrives in the red time, and 8.5% energy savings when the vehicle arrives in the green time The proposed method also works for different speed and time the vehicle initially enters the DSRC range.

5. Eco-Approach and Departure Strategies along Actuated Signalized Corridor

The eco-approach and departure (EAD) system designed for signalized intersections has been proven to be effective for energy saving effect. However, most existing applications focused on trajectory optimization for a single intersection. When driving along corridors, such applications will only reach intersection-based optimized performance and perform suboptimal corridor-wise. With the wide exploited actuated signals, in this chapter, we present an EAD strategy along actuated signalized corridors. We first extend the stochastic SPaT model in Chapter 3 into corridor level, and then proposed an adaptive EAD strategy for vehicles driving at actuated signalized corridors, which can achieve the corridor-wise minimum expected energy. Using SPaT data from consecutive actuated signals, geographic, and vehicle dynamic information, the algorithm could derive the most energy-efficient speed profile for vehicles to follow. This technique was validated using real-world signal data collected from the Innovation Corridor in the city of Riverside, CA and tested in a simulation environment, and achieved an energy savings of 8.8% - 11.8% compared to baseline and 4.4% - 6.2% compared to intersection-based EAD algorithm for the study actuated signal corridor.

5.1 Introduction

As mentioned in Chapter 1, the majority of the EAD applications were developed based on a single intersection, in which the vehicle will only operate based on the SPaT information from the nearest signal. Some eco-driving research considered SPaT messages from

multiple intersections along a corridor for a coordinated plan. Wu et al. developed an EAD algorithm along signalized corridors considering different powertrain characteristics (*20*). In this work, SPaT information from all the signals was considered and a reachable region was constructed using the received fixed-timing signals. Zhang et al. designed a reinforcement learning-based EAD strategy for EV on a signalized corridor and applied the twin delayed deep deterministic policy gradient algorithm to train the operations of the vehicle (*36*). Li et al. conducted a simulation-based analysis to study the potential safety, mobility, and environmental impacts of EAD and concluded that the application showed great potential in reducing the vehicles' energy consumption, but the safety benefits were heavily scenario dependent (*37*). Asadi proposed an optimization-based control algorithm aiming to arrive at green light with minimal use of braking and maintain a safe distance between vehicles (*38*). In (*39*), an EAD at signalized corridors was developed and a safety analysis was performed that showed higher penetration had positive effects on network-wide safety benefits. Han et al proposed an energy-efficient and safe EAD strategy considering speed varying desired time headway policy (*40*). Sun et al. introduced the concept of 'effective red-light duration' to describe the feasible passing time through signalized intersections and solved the optimal control problem using dynamic programming (*41*). Ozatay et al. solved the EAD problem in two stages, where the first stage determined the traffic light arrival times and the second stage calculated the optimal velocity profile using the vehicle models and traffic light arrival times (*42*). Lin et al. presented a fuel-saving strategy for traveling between two signalized intersections and solved the optimal control problem (OCP) using the Legendre pseudo-spectral (LPS)

method (*43*). Nunzio presented a three-stage EAD, green window selection, energy calculation, and speed advisory and the method was compared with Dynamic programming for computational time and energy consumption (*44*). In (*45*), a multi-stage optimal approach was proposed to minimize fuel consumption, and field experiments were carried out for comparative analysis. Yang et al. proposed an EAD model and tested it at different system market penetration rates (MPRs) (*46*). Although reaching a great energy-saving performance for corridor-wise eco-driving, the above studies are conducted under the assumption that the intersections are only equipped with fixed-timing signals. However, in real-world traffic in the U.S., about 70% of the intersections are controlled by actuated signals. Compared to fixed timing signals which provide reliable SPaT information in advance, actuated signals perform dynamic phase extension or even phase skipping depending on the real-time traffic conditions, which makes it challenging to predict the future SPaT status. The existing methods will not provide energy efficient strategy due to the highly unreliable SPaT information when applied to the actuated signalized corridors.

In this chapter, we proposed a graph-based trajectory planning algorithm that solves the optimal speed trajectory solution for EAD on an actuated signalized corridor using the dynamic programming approach. Regarding the uncertainty of the SPaT information, we trained a probabilistic model using historical SPaT data to infer the potential SPaT updates (and their probability) in future time steps given the current SPaT status. The algorithm then considers the SPaT messages from all the following actuated signals in a corridor and computes the speed profile that achieves the global minimum expected energy consumption.

5.2 Problem Statement

In this proposed multiple intersection connected eco-driving framework, four types of information are fed into the algorithms to derive the most energy-efficient solution for the equipped vehicle, as shown in Figure 5.1. Their definitions are as follows:

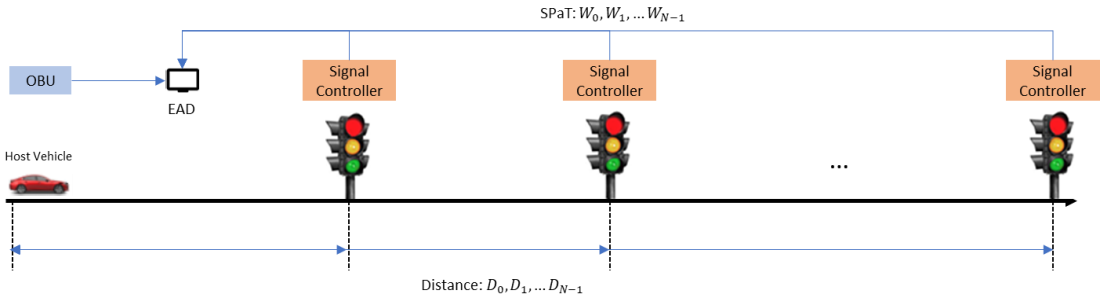

Figure 5.1. Illustration of corridor EAD for actuated signals.

1. Distance to the following intersections ($D_0, D_1, \dots D_{N-1}$): the road distance from the current GPS location to the stop line of following intersections from closest (D_0) to farthest (D_{N-1}).

2. Vehicle speed (V): the current speed of the vehicle, measured by on-board diagnostics (OBD) or GPS devices.

3. Time (t): current time stamp.

4. SPaT information of the following intersections ($W_0, W_1, \dots W_{N-1}$): the status of traffic signals with the phase status ($W_{i,P}$), current time in the phase ($W_{i,T}$) and estimated minimum ($W_{i,Min}$) and maximum $W_{i,Max}$ time-to-change for the current signal phase of all intersections in the corridor. These 4 types of SPaT information are provided in most signal controllers with SPaT broadcasting functions, and form a sample corridor EAD as shown in Figure 5.2.

For the previous works where EAD is applied to a single intersection, both Dedicated Short-Range Communications (DSRC) and C-V2X are commonly used as the V2I communication method. However, in our corridor EAD framework with multiple intersections, DSRC is no longer considered due to the limited communication range and the need for SPaT messages from all intersections at the same time. As the corridor-based method aims to achieve a global minimum on energy consumption, it might underperform in terms of energy consumption at a specific intersection compared to the single intersection EAD algorithm. There are three major challenges in this problem: 1) how to utilize the information of all the signals and manage the uncertainty of all the actuated signals to develop an adaptive strategy, 2) how to balance the time, speed and energy consumption in the objective function and 3) how to find the global minimum-energy trajectory for eco-driving instead of local minimum trajectories intersection-by-intersection. In the following subsections, we first discuss the stochastic SPaT model that can accommodate the model framework. Then, we will describe how we balance the speed and time with energy consumption to achieve the optimal solution. Finally, we propose a dynamic programming (DP) based model framework to efficiently investigate the optimal solution.

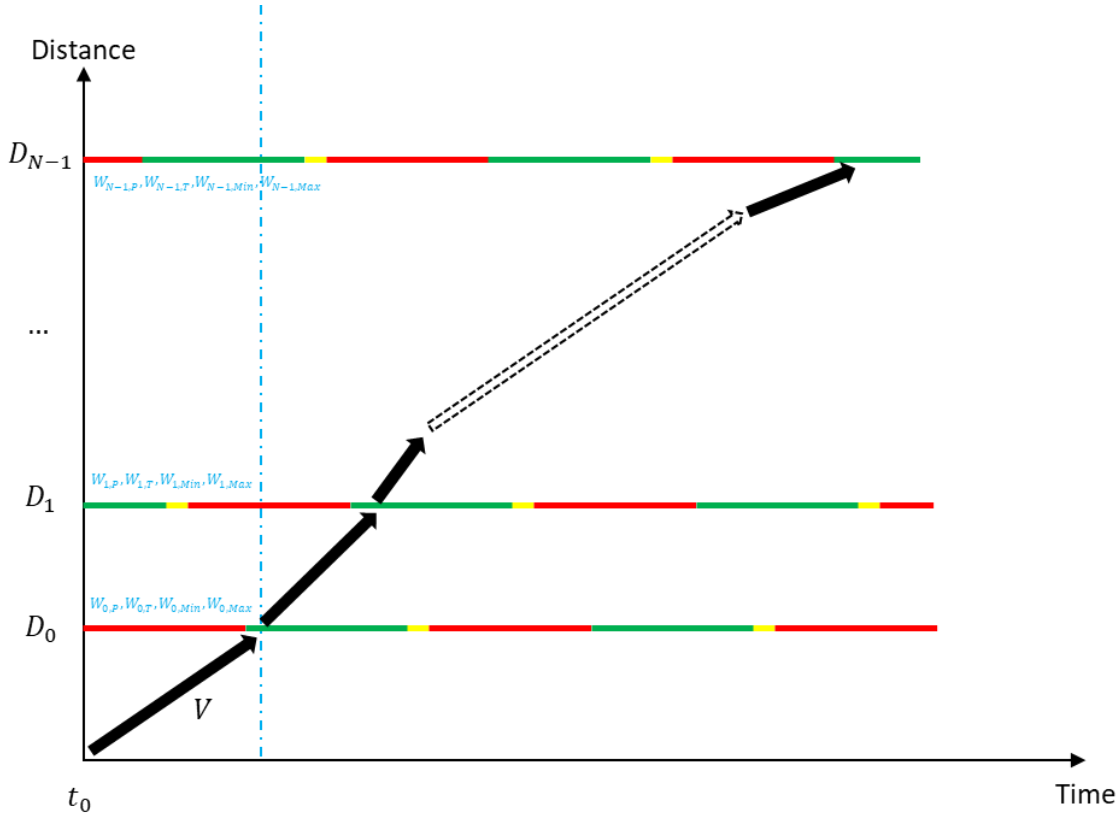

Figure 5.2. Sample trajectories of corridor EAD for actuated signals.

5.3 Statistical SPaT Model for Corridor-wised Actuated Signals

Similar to Chapter 3 where SPaT data id defined, we can define the SPaT state W_i for signal $i = 1, 2, \ldots N-1$ as a set of four parameters: current phase $W_{i,P}$, elapsed time in the current phase(sec) $W_{i,T}$, estimated minimum time to change for the current phase(sec) $W_{i,Min}$, and estimated maximum time to change for the current phase(sec) $W_{i,Max}$. Note that we assume that the occurrences of SPaT messages from any two intersections are independent, meaning that each signal state in the *i*th intersection could happen together with all the signal states in the *j*th signal. The corridor level SPaT graph can be expressed as below:

$$For\ each\ intersection, signal\ state\ graph\ =\ (Vertex, Edge) \qquad (5.1)$$

$$\text{with } Vertex = \{W_i = (W_{i,P}, W_{i,T}, W_{i,Min}, W_{i,Max})\} \text{ for i} = 1 \dots N-1$$

$$Edge = \{(W_i, W_j)\} \text{ for connected } i\text{th and } j\text{th signal state}$$

$$\sum_{\forall j} Weight_{W_i \to W_j} = 1$$

Note that we are assuming that the signal states between any two signals are independent of each other, hence the possible values of j for $W_i \to W_j$ in Equation (5.1) will be all possible states of *j*th intersection. If the two signal states are dependent on each other, the value of j will be a subset of all signal states of intersection j.

5.4 Time and final speed penalty in terms of energy consumption

In this chapter, our goal is to achieve the most energy-efficient trajectories globally given the state of the vehicle and all the signal information in the corridor. However, the time spent and final speed at the end of the study intersection should also be considered, as longer travel times lead to unwanted travel delay, and low final speed means a slow start for the remaining trip. To normalize the energy, time and final speed values for a fair comparison, we propose a method to convert travel time and final speed of the vehicle into energy consumption penalties, so that the whole system can be optimized based on one global measurement.

To estimate the penalty for time delay t_d in terms of energy consumption, we simply formulate a chase problem to calculate how much additional energy is needed to catch up the delay. Assume vehicle *A* passes the intersection at time 0 with target speed v_t, and keeps this speed for the rest of trip. Another vehicle B passes the intersection at time t_d with

target speed v_t, and would like to chase A, which has traveled $v_t t_d$ already. We then construct a trajectory for vehicle *B* to catch up *A* as early as possible. This trajectory starts with an acceleration segment to close the gap, followed by a possible constant-speed segment if the speed reaches the speed limit, and ends up with a deceleration segment to ensure the speed goes back to v_t when vehicle *B* meets *A*. We then calculated the additional energy consumption required for *B* (defined as P_{t_d}) in this process as the penalty for time delay t_d.

To estimate the penalty for low final speed v_f (i.e. $v_f < v_t$) in terms of energy consumption, we also formulate a chase problem to calculate how much additional energy is needed to catch up the delay due to the initial speed difference. Assume vehicle *A* passes the intersection at time 0 with target speed v_t, and keeps this speed for the rest of the trip. Another vehicle B passes the intersection at the same time with lower speed v_f. Similar as the time delay case, we need to construct an acceleration-constant speed-deceleration trajectory for vehicle *B* to meet *A* again with the same speed. We then calculated the additional energy consumption required for *B* (defined as P_{v_f}) in this process as the penalty for lower final speed v_f.

5.5 Pseudocode for Table Construction of Trajectory Planning

This problem is formulated into a multiple-source single-destination shortest path problem. It can be solved using a variation Dijkstra algorithm in which two nodes are linked only if their time states are consecutive. Assuming there are total of *n* intersections in the corridor, the proposed framework will solve for the *M* and *x* for the n_{th} intersection first where the SPaT message only contains information from its own. After that, the *M* and *x* for the *(n-*

*1)*th intersection will be constructed with final state defined as the initial state of the n_{th} intersection and *W* contains information from two intersections, for example:

$$M_N(D = 0, V, W_{N-2}, W_{N-1}, 1) = M_{N-1}(D = D_{max}, V, W_{N-1}, 1) \quad (5.2)$$

Using similar approaches, the cost and action corresponding to each state in the corridor could be calculated.

The pseudocode for table construction of trajectory planning is shown below.

Input: Signal transition graph with probability weights (*M*), intersection distance (*D*), target speed (v_t), and speed limit (v_l)
Output: Speed advisory table for trajectory planning
For intersection N:
1: Initialize $table(D, V, W_{N-1}, 2) = null$;
2: Initialize all final states, and add speed and time penalty,
3: $table(D = 0, V, W_{N-1} = green\&yellow, 1) = P_V$
4: $table(D = 0, V, W_{N-1} = green\&yellow, 2) = V$
5: for D = 0 to $D_{max,N-1}$
6: for V = 0 to $V_{max,N-1}$
7: for $t_1 = \forall SPaT_{N-1}$
8: Find possible t_2 after t_1 and calculate transition energy
9: update table if $table(D, V, W_{t1,N-1}, 1) < table(D, V, W_{t2,N-1}, 1) + H$
10: Return $table(D, V, W_{N-1}, 2)$

For intersection N-i, i = 2, …N:
1: Initialize $table(D, V, W_{N-i}, \dots W_{N-1}, 2) = null$;
2: Initialize all final states, and add speed and time penalty,
3: $table(D = 0, V, W_{N-i}, \dots W_{N-1}, 1) = table(D = D_{max}, V, W_{N-i-1}, \dots W_{N-1}, 1)$
4: $table(D = 0, V, W_{N-i}, \dots W_{N-1}, 2) = table(D = D_{max}, V, W_{N-i-1}, \dots W_{N-1}, 2)$
5: for D = 0 to D_{maxN-i}
6: for V = 0 to V_{maxN-i}
7: for $t_1 = \forall SPaT_{N-i}$
8: Find possible t_2 connected to t_1 for Intersection N to N-i and calculate transition energy *H*
9: update table if $table(D, V, W_{t1N-i}, \dots, W_{t1N}, 1) < table(D, V, W_{t2N-i}, \dots, W_{t2N}, 1) + H$
10: Return $table(D, V, W_{N-i}, \dots W_{N-1}, 2)$

The construction of the trajectory planning table starts from the downstream to the upstream intersection, and utilizes the SPaT information from every signal in the downstream of the corridor.

5.6 Case Study and Results

We designed two scenarios, fixed timing signalized corridor and actuated signalized corridor, to test the proposed algorithm for its energy saving effect in different conditions. Simulations are conducted in MATLAB to test the proposed method and compare it with the baseline. Table 5.1 below shows the assumptions for all the simulations in the red and green light phase.

Table 5.1. Simulation Assumptions and Parameters.

n	Number of intersections	2
D	Distance of each intersection	400 m
v_t	Targeted speed of the host vehicle at intersection	10 m/s
v_{max}	Maximum speed	18 m/s
v_{min}	Minimum speed	0 m/s
a_{max}, - a_{min}	Maximum and minimum acceleration	2 m/s^2
Δd_{TL}, Δt, Δv	Minimum interval in the state parameters	1

5.6.1 Simulation Results for Fixed Timing Signalized Corridor

The signalized corridor is designed to be equipped with two fixed timing signals. This scenario is designed to show that our algorithm will still perform effectively under fixed timing signals. Both signals have a full cycle of 80 sec, with 36 sec green, 4 sec yellow,

and 40 sec red. The host vehicle is allowed to pass the intersection during green and first 3 sec of yellow phase due to safety concerns.

We propose three other algorithms to prove the energy efficiency performance of the proposed corridor-based EAD algorithm, 1) intersection-based EAD algorithm, 2) human driver with 2 m/s^2 maximum acceleration and 3) human driver with 1 m/s^2 maximum acceleration. The intersection-based EAD algorithm uses the same optimization function as corridor-based EAD algorithm but without SPaT information of the following intersection. The baseline driver models are developed as follows: when the host vehicle enters the study zone, the vehicle will first accelerate to the maximum speed using constant maximum acceleration, then gradually decelerate at constant deceleration after reaching the safety distance until the vehicle stops at the intersection. The safety distance is defined as the shortest distance the vehicle needs to stop at the intersection with the maximum deceleration. If the traffic signal changes to green phase in this process, the vehicle will immediately accelerate with the maximum acceleration and pass the intersection as soon as possible. The two cases of human drivers are to simulate two kinds of drivers in the real world.

To compare the energy consumption between the proposed and baseline method, the simulation is conducted on a total of three full cycles (180 sec) with the host vehicle entering the corridor at every two seconds till 120 seconds (60 runs). We calculated the mean raw energy and time consumption for all the 60 runs and then added the penalty energy for speed and travel time to count for the time and speed difference. Raw energy is defined as the energy consumption before adding energy penalties for final speed and time.

Table 5.2 & 5.3 show the average energy consumption before and after energy penalty is added, and travel time between the four methods with different initial speed. The saving percentage is calculated based on the Baseline 1m/s^2 case.

Table 5.2. Simulation results for four methods with initial speed equals 1 m/s in fixed timing signalized Corridor (Energy: kJ, Time: sec)

	Raw		***With Penalty***		***Savings***	
	Energy	Time	Energy	Time	Energy	Time
Corridor EAD	44.4	67.0	44.4	67.0	68.7%	23.2%
Intersection EAD	50.6	67.5	52.2	67.5	63.2%	22.6%
Baseline 2m/s^2	69.3	68.4	78.2	68.4	45.0%	21.6%
Baseline 1m/s^2	66.1	87.2	142.1	87.2	0.0%	0.0%

Table 5.3. Simulation results for four methods with initial speed equals 18 m/s in fixed timing signalized Corridor (Energy: kJ, Time: sec)

	Raw		***With Penalty***		***Savings***	
	Energy	Time	Energy	Time	Energy	Time
Corridor EAD	30.6	63.0	30.6	63.0	71.1%	20.6%
Intersection EAD	32.6	63.6	34.6	63.6	67.3%	19.8%
Baseline 2m/s^2	43.5	64.4	52.3	64.4	50.6%	18.8%
Baseline 1m/s^2	42.6	79.3	105.8	79.3	0.0%	0.0%

As can be seen from the two tables, the corridor-based EAD algorithm performs the best in all four methods. When initial speed is 1m/s, the corridor EAD reaches 68.7% and 23.2% in energy and time savings respectively compared to baseline with 1 m/s^2 acceleration. The intersection EAD has a closer performance to corridor EAD with 12.25% more energy consumption and 0.74% more time consumption. The baseline with 2m/s^2 has a similar time consumption, but due to its aggressive acceleration strategy, the energy consumption

turns out to be larger than the previous two methods. The 1m/s^2 baseline has a smaller energy consumption than the other baseline, but its time consumption is significantly larger, causing the total energy with penalty to be the highest among all four algorithms.

When initial speed is 18 m/s, due to the higher initial kinetic energy, all the four algorithms finish the same route with lower energy and time consumption. The corridor EAD reaches 71.1% and 20.6% in energy and time savings respectively compared to 1m/s^2 baseline. Due to the fixed phase planning of the two signals, the corridor EAD algorithm can always reach the destination with target or higher speed, causing no energy added for speed penalty.

To better understand the benefit of the corridor EAD algorithm, we plot the sample trajectories between the corridor-based EAD, intersection-based EAD and Baseline 2 m/s^2 in Figure 5.3 below. Note that in each figure, we overlay the results of all test vehicle trajectories with different starting time (with 2 seconds as the interval), but each trajectory does not interact with each other as we only focus on single EAD vehicle in this algorithm. As shown in the figure, the corridor EAD algorithm avoids all the red signal phases at both intersections while maintaining a high speed when passing through the destination. The intersection-based EAD also avoids all stops at red signal phase, but the vehicle tends to quickly accelerate to full speed to save traveling time passing the first intersection as it does not have any SPaT information from the following intersections. That strategy is efficient in both mobility and energy if the vehicle faces another green in the next intersection. However, if the next signal is in red when the intersection-based EAD vehicle arrives, it has to decelerate to avoid a stop. In this case, the quick-acceleration strategy at the first intersection is not as efficient in energy. As a comparison, the corridor-based EAD

algorithm can optimize the speed trajectory for the entire trip and choose to slowly accelerate to pass the second intersection using similar time as the intersection-based EAD but with lower energy consumption. The $1m/s^2$ baseline performs the worst with deceleration and stops at the red signal which wastes time and energy.

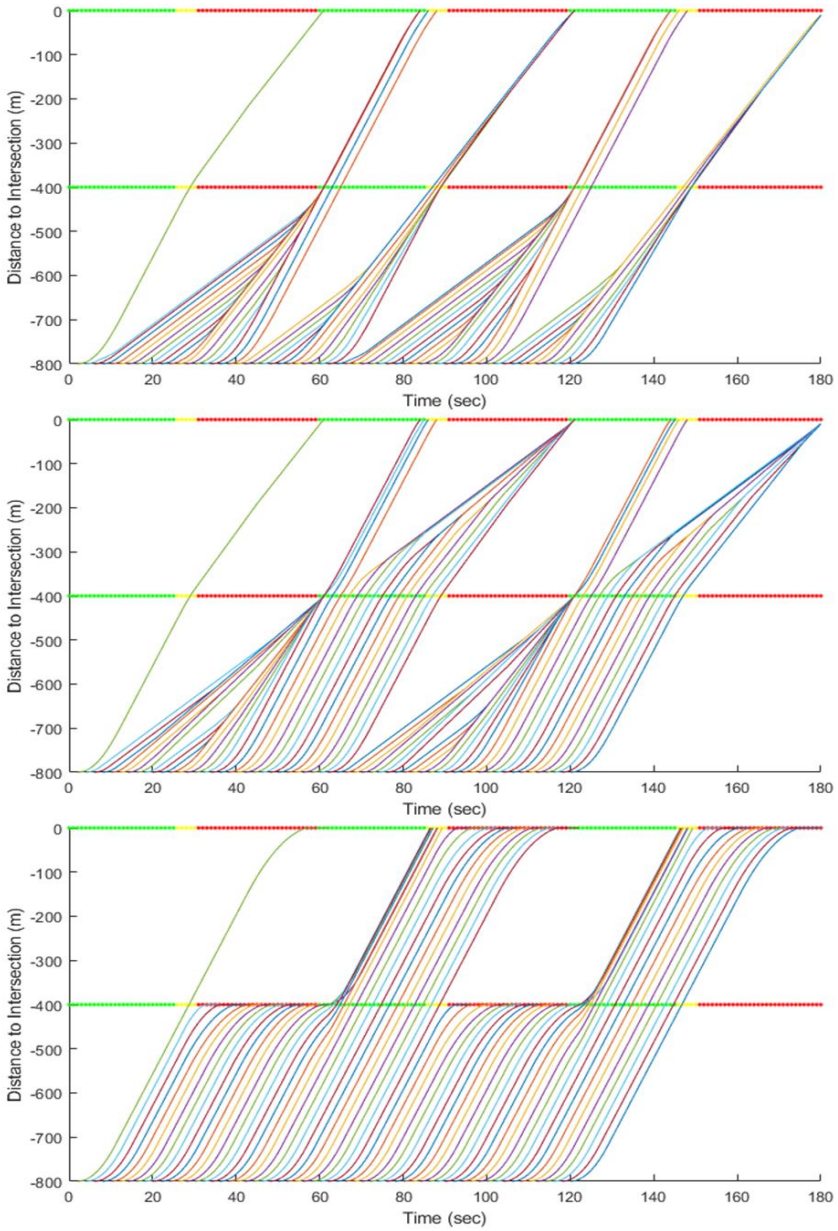

Figure 5.3. Sample trajectories of Corridor EAD (up), intersection-based EAD (middle), and baseline 2 m/s^2 (down) for initial speed equals 1m/s at fixed signalized corridor.

5.6.2 Simulation Results for Actuated Timing Signalized Corridor

For the actuated signalized corridor, we used the same two-intersection simulation network but this time with real-world SPaT data. The SPaT data applied in the algorithm were collected from the Innovative Corridor, eastbound of the University Avenue, intersections University Ave @ Cranford Ave and University Ave @ Chicago Ave in Riverside, CA. The data were preprocessed so that only the 12pm-2pm time period between July 1st, 2021 to July 31st, 2021 was included. The certain time period enables less phase plan variation and uncertainty in the graph construction, which makes the suggested speed more accurate for energy saving. All the time parameters are rounded to integers to decrease the number of nodes in the SPaT graph. The minimum intervals for the state parameters are selected to be one so that the computational time is acceptable for real-time application. We applied the four methods to two scenarios: one has intersection distances of 400 & 400 for the first and second intersection, respectively, the second scenario is equipped with distances of 400 & 100. To compare the energy consumption between the proposed and baseline method, a total of 60000 seconds of historical SPaT messages at each intersection of the corridor are tested with different phase-entering times and initial velocities. Penalty energy for speed and travel time is also added to count for the time and speed difference.

Scenario #1

Table 5.4 & 5.5 show the average energy consumption before and after energy penalty is added, and travel time between the four methods with different initial speed. The saving percentage is calculated based on the Baseline $1 m/s^2$ case.

Table 5.4. Simulation results for four methods with initial speed equals 1 m/s in actuated timing signalized Corridor Scenario #1 (Energy: kJ, Time: sec)

	Raw		***With Penalty***		***Savings***	
	Energy	Time	Energy	Time	Energy	Time
Corridor EAD	58.7	78.8	66.6	78.8	**11.8%**	3.5%
Intersection EAD	59.9	79.5	69.9	79.5	7.4%	2.6%
Baseline 2m/s^2	65.9	76.6	72.6	76.6	3.9%	**6.2%**
Baseline 1m/s^2	60.8	81.6	75.6	81.6	0.0%	0.0%

Table 5.5. Simulation results for four methods with initial speed equals 18 m/s in actuated timing signalized Corridor Scenario #1 (Energy: kJ, Time: sec)

	Raw		***With Penalty***		***Savings***	
	Energy	Time	Energy	Time	Energy	Time
Corridor EAD	37.9	74.3	44.5	74.3	**8.8%**	-1.0%
Intersection EAD	38.0	75.2	47.5	75.2	2.6%	-2.3%
Baseline 2m/s^2	39.9	72.4	46.6	72.4	4.4%	**1.5%**
Baseline 1m/s^2	37.4	73.5	48.8	73.5	0.0%	0.0%

As can be seen from the two tables, without sacrificing travel time, the energy consumption of the proposed corridor EAD algorithm is always the minimum among all four algorithms, reaching 11.8% and 8.8% for initial velocity 1 m/s and 18 m/s respectively. A smaller energy saving for larger initial speed is due to higher initial kinetic energy and less space to adjust the speed trajectory of the host vehicle. When initial speed is 18 m/s, the baseline

$2m/s^2$ consumes slightly more raw energy than the intersection EAD, but less overall energy after penalty is added, which shows the importance of cooperatively utilizing SPaT data from multiple consecutive intersections. Compared to fixed timing signals, the overall energy and time saving are less significant due to the highly uncertainty of the SPaT messages and large amount of SPaT combinations.

We then split the trajectory into two subparts: before the vehicle passes the first and second intersection respectively, to analyze the energy and time consumption between the four methods. As can be seen from Tables 5.6 & 5.7, the Intersection EAD method keeps the energy consumption lowest at the first half of the trajectory, but its lower reaching speed increases the energy consumption of the first half of the trajectory and drags down the total energy saving. The Corridor EAD method consumes more energy in the first half of the trajectory, 5.4% for the 1m/s initial speed and 32.9% for the 18m/s initial speed scenarios respectively, compared to the baseline with $1m/s^2$ acceleration. But in return, it reaches higher end speed with 16.1 m/s and 15.9 m/s at the first intersection with similar travel time. The start with higher speed for the second half of the trajectory will later on help the host vehicle to reach an overall minimum energy consumption when considering both speed and travel time, which proves the effectiveness of the Corridor EAD method. It's worth mentioning that the faster travel time during the first intersection compared to the second intersection is due to the shorter red light duration in the first intersection.

Table 5.6. Subparts raw energy and time results for four methods with initial speed equals 1 m/s in actuated timing signalized Corridor Scenario #1 (Energy: kJ, Time: sec)

	First Intersection			***Difference***		***Second Intersection***		***Difference***	
	Energy	Time	Speed	Energy	Time	Energy	Time	Energy	Time
Corridor EAD	38.7	31.8	**16.1**	-5.4%	6.4%	20.1	47.1	**16.8%**	1.6%
Intersection EAD	34.4	31.7	11.3	**6.2%**	6.5%	25.5	47.8	-5.7%	0.1%
Baseline 2m/s²	40.1	29.9	14.3	-9.4%	11.9%	25.7	46.9	-6.6%	2.1%
Baseline 1m/s²	36.7	33.9	13.9	0.0%	0.0%	24.1	47.8	0.0%	0.0%

Table 5.7. Subparts raw energy and time results for four methods with initial speed equals 18 m/s in actuated timing signalized Corridor Scenario #1 (Energy: kJ, Time: sec)

	First Intersection			***Difference***		***Second Intersection***		***Difference***	
	Energy	Time	Speed	Energy	Time	Energy	Time	Energy	Time
Corridor EAD	17.7	27.1	**15.9**	-32.9%	-4.6%	20.2	47.1	**16.0%**	1.4%
Intersection EAD	12.1	27.3	10.7	**9.6%**	-5.1%	26.0	47.9	-8.0%	-0.3%
Baseline 2m/s²	14.3	25.9	14.3	-7.1%	0.2%	25.6	46.8	-6.6%	2.1%
Baseline 1m/s²	13.3	25.9	13.8	0.0%	0.0%	24.0	47.8	0.0%	0.0%

Figure 5.4 below compares the sample trajectories between the corridor-based EAD, intersection-based EAD and Baseline 2 m/s^2. As shown in the figure, the corridor EAD algorithm avoids most red signal phases on both intersections and can reach a higher speed when passing through the destination. Due to the unreliable phase duration, the signal might change to red phase when it's closer to the intersection, causing the host vehicle to occasionally slowly decelerate and stop at the intersection. On the other hand, due to the lack of knowledge of SPaT information of the second intersection, the intersection-based

method will accelerate faster to pass the first intersection, which causes a higher probability of stopping at the first intersection. This faster acceleration is also sometimes unnecessary since the vehicle might have to decelerate at the second intersection to wait for the green signal. As can be seen from the red phases at the first intersection that are circled in red, the corridor-based EAD could start decelerating slightly earlier compared to the intersection-based EAD, due to the processing of SPaT information from both intersections. This also results in a faster passing speed at the first intersection. On the other hand, the baseline performs the worst with frequent stops at both the first and second intersections, which wastes both time and energy. It's also worth noticing that unlike the fixed timing signal scenarios which both corridor and intersection-based methods could avoid any stop at the intersections, the actuated signals have unreliable signal phase durations, which causes the vehicles to occasionally stops at the intersection even when EAD strategies are applied. Meanwhile, due to the higher uncertainty in predicting the SPaT information from the far-end intersection, the corridor-based EAD is more short-sighted compared with the fixed-timing case. It is not likely to have more acceleration and deceleration due to frequent SPaT updates. However, the corridor-based method still outperforms the other two methods with least stops and energy consumption.

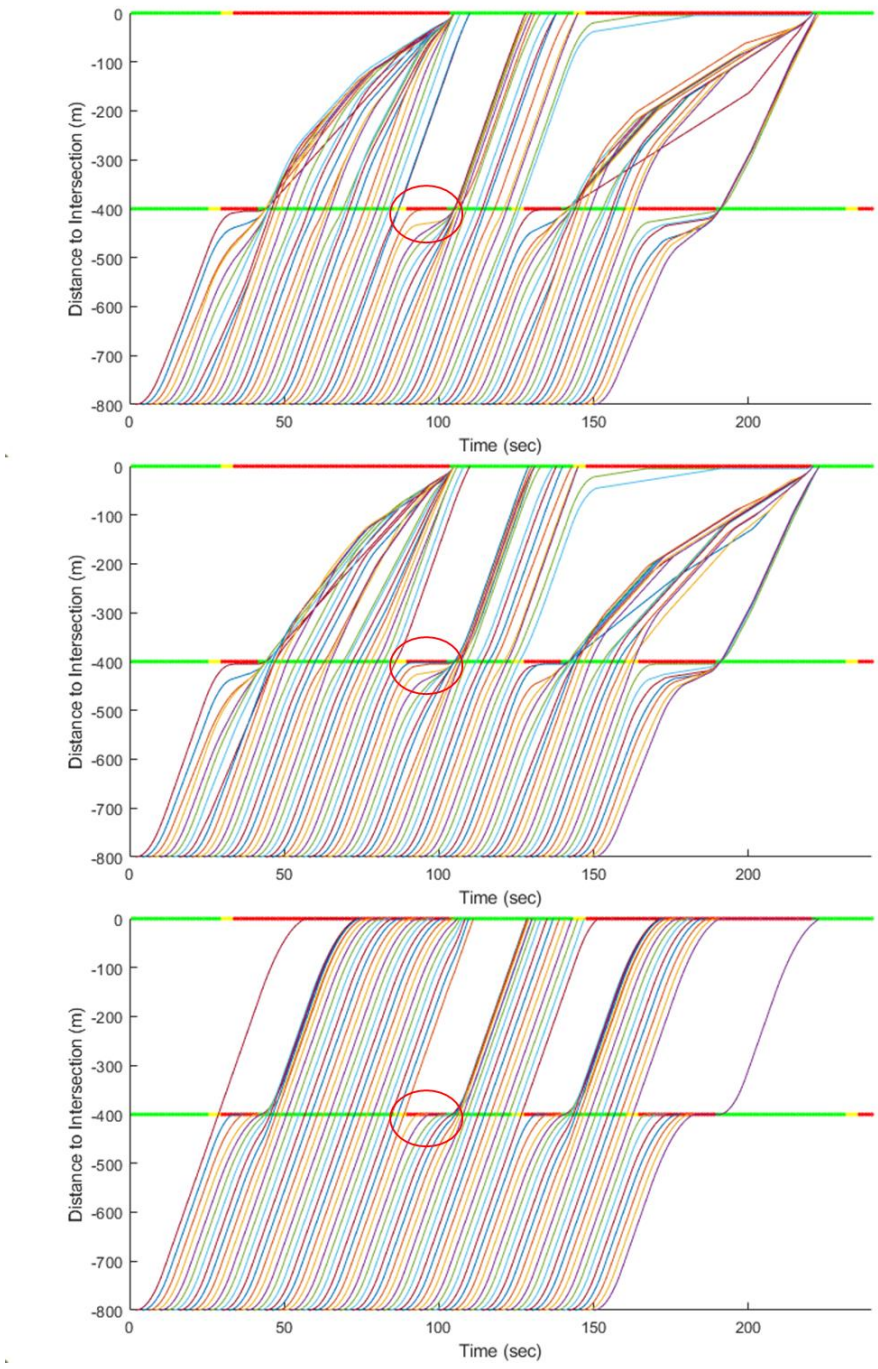

Figure 5.4. Sample trajectories of Corridor EAD (up), intersection-based EAD (middle), and baseline 2 m/s^2 (down) for initial speed equals 1m/s at Scenario #1 actuated signalized corridor.

Scenario #2

The next test scenario is designed to have the same distance (400) at the first intersection but a much shorter distance (100m) at the second intersection to compare the strategy difference of the Corridor EAD to the first scenario. Table 5.8 & 5.9 show the average energy consumption and travel time between the four methods with the saving percentage calculated based on the Baseline 1m/s^2 method. When the initial speed is 1m/s, both the Corridor EAD and the Intersection EAD are performing significantly better than the Baseline 1m/s^2, reaching 27.8% and 26.3% energy savings respectively. The Baseline 2m/s^2 finishes the trajectory the fastest as expected but consumes the most raw energy in the trip. The Baseline 1m/s^2 consumes less raw energy compared to the other baseline case, but when we count in the extra travel time and lower final speed, the overall performance becomes the worst. Similar to scenario # 1, the Corridor EAD method performs the best among the four in terms of overall energy consumption. The energy difference between the Corridor and Intersection EAD methods gets smaller due to the shorter overall distance and lower overall energy consumption. Some sample trajectories are shown in Figure 5.5, where both Corridor EAD and Intersection EAD have shown great ability to predict the potential red light and control the vehicle to pass the intersection without a long wait at the intersection. Similar to Scenario #1, the Corridor EAD algorithm performs slightly better at the first intersection where less deceleration and higher final speed could be reached for overall lower energy consumption.

Table 5.8. Simulation results for four methods with initial speed equals 1 m/s in actuated timing signalized Corridor Scenario #2 (Energy: kJ, Time: sec)

	Raw		***With Penalty***		***Savings***	
	Energy	Time	Energy	Time	Energy	Time
Corridor EAD	47.4	62.2	53.4	62.2	**27.8%**	6.5%
Intersection EAD	47.8	62.8	54.6	62.8	26.3%	5.6%
Baseline 2m/s^2	56.3	61.3	62.1	61.3	16.0%	**7.9%**
Baseline 1m/s^2	50.3	66.5	74.0	66.5	0.0%	0.0%

Table 5.9. Simulation results for four methods with initial speed equals 18 m/s in actuated timing signalized Corridor Scenario #2 (Energy: kJ, Time: sec)

	Raw		***With Penalty***		***Savings***	
	Energy	Time	Energy	Time	Energy	Time
Corridor EAD	25.9	57.6	31.7	57.6	**16.3%**	0.6%
Intersection EAD	25.7	58.5	33.1	58.5	12.4%	-0.9%
Baseline 2m/s^2	30.4	56.7	36.2	56.7	4.3%	**2.2%**
Baseline 1m/s^2	26.9	58.0	37.8	58.0	0.0%	0.0%

Next, we split the trajectory again into two subparts like scenario #1, with raw energy and speed differences shown in Table 5.10 & 5.11. The Intersection EAD performs the best in the first half of the trajectory, reaching energy savings of 9.8% and 18.4% for initial speeds

1m/s and 18m/s respectively. The Corridor EAD consumes more energy than the Intersection EAD with similar travel time in the first half. But it reaches a higher travel speed to start with the second half of the trajectory and consumes the least amount of energy for the second half and overall trajectory. It is worth noticing that compared with Scenario #1, the Corridor EAD in Scenario # 2 reaches a smaller end speed (14.2 vs 16.1, 13.7 vs 15.9) after the first intersection. This finding also shows that the Corridor EAD can find the optimal intermediate speed when transitioning from the first intersection to the second.

Table 5.10. Subparts raw energy and time results for four methods with initial speed equals 1 m/s in actuated timing signalized Corridor Scenario #2 (Energy: kJ, Time: sec)

	First Intersection			***Difference***		***Second Intersection***		***Difference***	
	Energy	Time	Speed	Energy	Time	Energy	Time	Energy	Time
Corridor EAD	35.8	31.8	**14.2**	6.0%	16.6%	11.5	30.4	**5.3%**	-6.1%
Intersection EAD	34.4	31.7	11.3	**9.8%**	16.9%	13.4	31.0	-10.2%	-8.5%
Baseline 2m/s²	41.6	34.2	14.3	-9.0%	10.6%	14.7	27.4	-20.9%	4.2%
Baseline 1m/s²	38.1	38.2	13.9	0.0%	0.0%	12.2	28.6	0.0%	0.0%

Table 5.11. Subparts raw energy and time results for four methods with initial speed equals 18 m/s in actuated timing signalized Corridor Scenario #2 (Energy: kJ, Time: sec)

	First Intersection			***Difference***		***Second Intersection***		***Difference***	
	Energy	Time	Speed	Energy	Time	Energy	Time	Energy	Time
Corridor EAD	14.1	27.2	**13.7**	4.9%	10.1%	11.8	30.4	**2.3%**	-9.0%
Intersection EAD	12.1	27.3	10.7	**18.4%**	9.8%	13.6	31.2	-12.2%	-11.8%
Baseline 2m/s²	15.7	30.2	14.3	-6.4%	0.2%	14.6	26.7	-20.9%	4.4%
Baseline 1m/s²	14.8	30.2	13.8	0.0%	0.0%	12.1	27.9	0.0%	0.0%

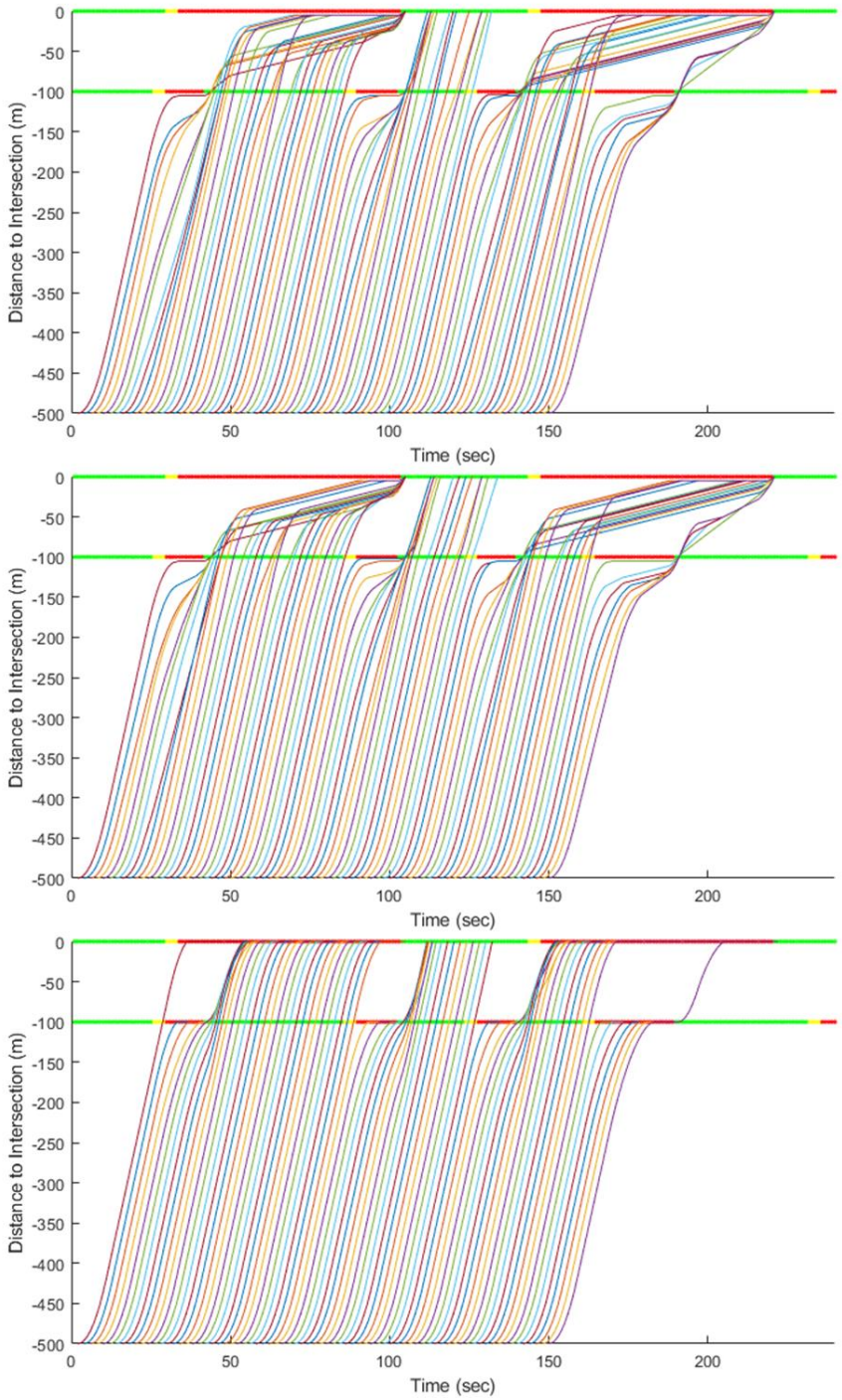

Figure 5.5. Sample trajectories of Corridor EAD (up), intersection-based EAD (middle), and baseline 2 m/s^2 (down) for initial speed equals 1m/s at Scenario #2 actuated signalized corridor.

5.7 Summary and Discussion

This chapter proposed an adaptive strategy for connected eco-driving towards actuated signalized corridors. Both energy and time comparisons are conducted between the proposed method and carefully designed baselines under different initial speeds and times. The validation results indicate the proposed DP corridor-based model can achieve the most energy-efficient trajectory, achieving an energy savings of 8.8% - 11.8% compared to the baseline and 4.4% - 6.2% compared to the intersection-based EAD algorithm, for the case when two intersections are 400m aparted. For the closely spaced intersections, the proposed corridor-based method can achieve higher energy savings up to 16.3% - 27.8%.

6. Connected Eco-Approach and Departure (EAD) Algorithm for Battery Electric Trucks

There has been increasing interest in adopting battery electric trucks (BETs) in recent years due to the high-efficiency and zero-emission operation of electric powertrain (*55*). However, current BETs still have a shorter range than their conventional diesel counterparts, which can cause range anxiety among BET drivers. To further improve the energy efficiency of BETs, and consequently, extend their range, we propose an eco-approach and departure (EAD) algorithm specifically designed for BETs to help these trucks approach and depart signalized intersections in an energy-efficient manner. In order to reduce the computation time for real-time execution, a machine learning model is trained to generate an approximate solution from the graph-based model. The proposed algorithm is evaluated in a microscopic traffic simulation network of urban freight corridors in Southern California with multiple connected and non-connected traffic signals. The simulation results show that the proposed EAD algorithm for BETs could help the host vehicle achieve an energy savings of 1.4% to 6.5% while maintaining a similar travel time under different simulation environment.

6.1 Introduction

Trucks play an important role in the U.S. economy by transporting large quantities of raw materials or finished goods over land among seaports, manufacturing factories, and distribution centers. According to the American Trucking Association, the trucking industry has hauled 10.93 billion tons of goods, about 72.2% of all freight transported in

the United States in 2021 (*47*). The blooming truck industry not only drives the economic growth of the country but has also become one of the largest contributors to greenhouse gas (GHG) emissions and air pollutants. According to the 2020 GHG emission report published by the U.S. Environment Protection Agency, the transportation sector has become the largest contributor (27%) to the U.S. GHG emissions (*48*). Among the 5 main transportation sectors, medium- and heavy-duty trucks, which make up only 4% of vehicles in the US, produce 26% of all the transportation GHG emissions (*48*). Meanwhile, air pollutant emissions from trucks have been a longstanding issue due to the potential health threats. Diesel exhaust from conventional trucks also contains particulates, sulfur dioxide, carbon monoxide, hydrocarbons, and various air toxics, which have significant negative health impacts to the communities in close proximity to truck routes or freight facilities.

As promising alternative to traditional diesel trucks, electric trucks have shown significant advantages on higher efficiency of the electric powertrain and lower running cost. According to the survey from the U.S. Department of Energy in 2019, the cost of a kWh of energy for a battery pack has decreased by more than 50% from 2013 to 2019 (*49*). The rapid development of the battery industry has also enabled a larger operation range of electric trucks while reducing the battery cost, but the electric trucking is still heavily restricted by the operational range due to the much less energy density of lithium-ion batteries than fossil fuel. The electric trucks would require mid-day recharging for long-distance transportation and cause additional delays to the trip.

Most existing EAD studies to date have focused primarily on internal combustion engine (ICE) vehicles, especially gasoline-powered passenger cars. Some works have studied the

impact of EAD on heavy-duty vehicles. Savkovic et al. evaluated the eco driving training process for professional truck drivers (*50*). In three months, fuel saving and CO_2 emission reduction has been increased from 3.27% to 6.37% and 36.39% to 63.75% respectively, showing that longer and consistent training could improve the energy saving benefit of heavy-duty trucks. Hauenstein et al. combined cooperative and energy-efficient driving and tested the eco-driving algorithm in a simulation environment during uphill driving (*51*).

According to the best knowledge of the authors, there is no study that evaluates the potential energy savings of EAD for electric trucks, and there is also limited research on the EAD performance comparison between electric trucks and diesel trucks. In this chapter, an EAD algorithm for battery electric trucks (BETEAD) is proposed, and microscopic simulations are conducted to evaluate the energy impact of BETEAD on host battery electric trucks. Using the data created by the graph-based trajectory planning algorithm, a random-forest model is trained to efficiently provide the optimal speed recommendation for the equipped electric truck for connected eco-driving. The BETEAD is also tested with different simulation environment and compared with diesel trucks to show the difference in energy savings.

6.2 Electric Truck Energy Consumption Model

The second-by-second energy consumption of an electric truck is calculated using the microscopic electric truck energy consumption model and parameters based on previous publication (*56*). The values of these parameters are listed in Table 6.1. For each time instance, t, the tractive power P_t is calculated as:

$$P_t = m_{ev} v_t a_t + 0.5 \rho C_d A v_t^3 + C_{rr} g m_{ev} v_t \quad (6.1)$$

where a is acceleration and v is truck velocity. m_{ev} is the mass of electric truck, defined as:

$$m_{ev} = m_v - m_e - m_{gb} + \frac{E_{battery}}{U} + m_m \quad (6.2)$$

The amount of battery discharge rate (Q_t) to meet the required tractive power P_t can be calculated according to (5.2):

$$Q_t = \frac{P_t}{\eta_m \times \eta_b \times \eta_w \times \eta_d} \quad (6.3)$$

Compared to the powertrain of a diesel truck, the electric truck can regenerate energy through regenerative braking, unlike diesel truck, which has zero tractive power when it is in coasting or braking mode, i.e. $a \leq a_{coast}$. The regenerated power (P_{regen}) from regenerative braking is calculated as:

$$P_{regen} = (P_t < 0) \times \eta_m \times \eta_b \times \eta_w \times \eta_d \quad (6.4)$$

Then, the total energy consumed per second can be calculated as:

$$P_{consumed} = Q_t + P_{regen} + P_{acc} \quad (6.5)$$

where P_{acc} represents electricity consumption by accessory load, such as powertrain support systems, climate control systems, and driver comfort features.

Instead of calculating the total energy consumption of the electric truck over the course of a trip, in this chapter we aim to characterize the energy consumption per second of the electric truck as a function of instantaneous speed and acceleration, which are the variables

that define a speed profile of the truck. To develop this model, we first compiled the previously estimated second-by-second energy consumption data of the electric truck from all the trips, along with their corresponding instantaneous speed and acceleration values, into a two-dimensional lookup table where speed and acceleration jointly define cells of the table and each cell stores the mean value of electric truck energy consumption for the corresponding speed and acceleration values. This lookup table was then used to create a surface plot, similar to the one in Figure 6.1. The resulting surface plot is not smooth and has some spikes, which are caused by the high variability in the energy consumption value, especially for cells with a limited amount of data. Therefore, we applied the thin-plate splines smoothing technique (*52*) to smooth out the surface plot. The final surface plot is shown in Figure 6.1. Note that there are some cells where the energy consumption value is negative. These cells have a negative value of acceleration, which means the electric truck is slowing down and its motor is in the regeneration mode. Thus, the energy consumption value is negative because energy is actually being generated under those circumstances.

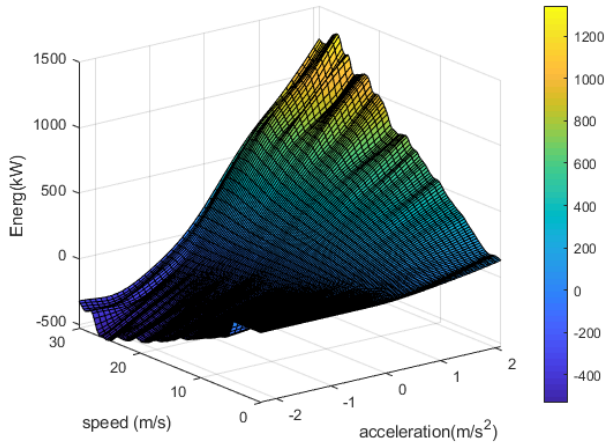

Figure 6.1 Energy consumption model used in the calculation

Table 6.1 Parameters Used for Electric Truck Simulation

	Parameter	Symbol	Value
Vehicle	Coefficient of drag	C_d	0.65
	Coefficient of rolling resistance	C_{rr}	.008
	Front area (m^2)	A	8.5
	Final drive efficiency	η_d	0.98
	Wheel efficiency	η_w	0.99
	Motor efficiency	η_m	0.88
	Battery efficiency	η_b	0.98
	Loaded vehicle mass (kg)	m_v	34545
	Accessory load for EV (kW)	AL_{ev}	2.8
	Engine mass (kg)	m_e	558
	Gearbox mass (kg)	m_{gb}	180
	Motor mass (kg)	m_m	432
Atmosphere	Air density (kgm^{-3})	ρ	1.161
	Gravity (ms^{-2})	g	9.8
Battery	Battery size (kWh)	$E_{battery}$	250
	Energy density (kWh/kg)	U	0.15

6.3 Graph-based and Random-forest Based Optimization Methods

Once we have a lookup table of electric truck energy consumption as a function of instantaneous speed and acceleration, we can apply it to design an optimal speed profile or trajectory for the truck. Two optimization methods were used—graph-based method and random forest-based method.

The graph-based trajectory planning algorithm in the previous chapters has shown good performance in optimizing the vehicle energy efficiency. However, the computation time for creating the graph and solving the shortest path problem is relatively long, which makes it unsuitable for real-time applications. As the computation time required by the Dijkstra's algorithm grows with the size of the graph, it makes real-time computation very challenging, especially when the EAD application must also deal with other data that it collects such as those from GPS and radar. In addition, an increase in communication range enabled by C-V2X that allows the EAD application to start planning vehicle trajectory far ahead of the intersection also increases the size of the graph, which renders real-time computation almost impossible. To accommodate the long computation time, the EAD application will have to increase the size of the time step Δt to be larger than the computation time required, which might reduce the energy savings that the EAD application could provide.

To help increase the computational efficiency of the EAD application, we employed a machine learning technique to learn the patterns of the solutions from the graph-based algorithm. A random forest model was trained using the data created by the graph-based algorithm (*53*). The input of the random forest model is the 3-D vehicle states (t-D-V), and the output is the optimal speed for the next time step. The random forest model consists of multiple decision trees, with each tree trained with a random subset of the created data. The predicted output of the random forest model is the average of the predictions from all the decision trees. As shown in Figure 6.2, the computation time of the random forest model

is not affected by the size of the graph, and performs on the order of magnitudes faster than the graph-based method.

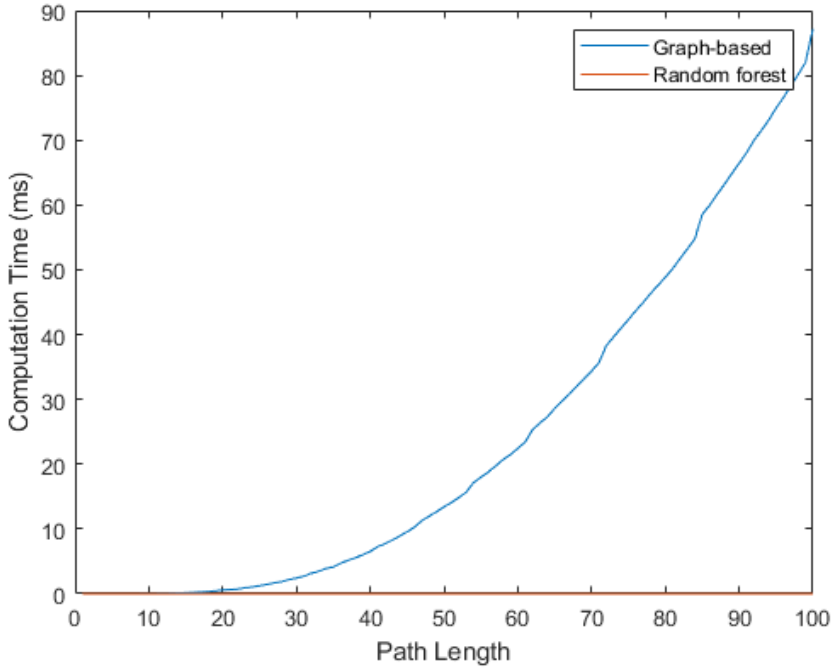

Figure. 6.2. Computational time comparison between graph-based and random forest-based methods

6.4 System Workflow

The BETEAD algorithm consists of two parts, offline and online. The offline part trains a random forest model using the output of the graph-based model. The online part is the one running in real-time on the electric truck that determines the optimal speed profile for passing through the intersection. As shown in Figure 6.3, the 3-D vehicle states (*t*-*D*-*V*) collected by the equipped vehicle are used in conjunction with vehicle dynamics information, which include the energy consumption model, to create the graph-based model. Using the energy consumption model for the electric truck, the optimal speed

profile can be calculated using the Dijkstra's algorithm, i.e. $v_{t+1} = G(t, D_t, v_t)$. The input-output pairs from the graph-based model are recorded, and later used as data to train the random forest model. Finally, the trained random forest model is used in the online part of the BETEAD algorithm for real-time computation of the optimal speed profile for the electric truck.

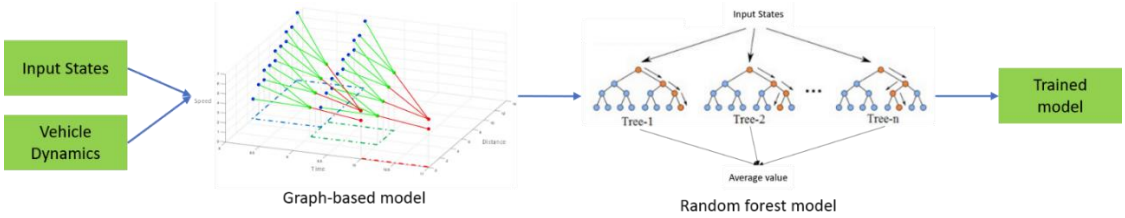

Figure 6.3. Offline process for developing the random forest model for use in the online BETEAD algorithm

Figure 6.4 shows the workflow of the online part of the BETEAD algorithm. Once the electric truck is within the communication range of the connected signalized intersection, real-time information about vehicle states (*t*-*D*-*V*) is collected by the system. Using data from an on-board radar or camera, the algorithm determines whether there is a preceding vehicle. If the preceding vehicle is too close, the algorithm will not start the trajectory planning as it may not be safe to do so. Otherwise, kinematic equations are used to determine whether the remaining green time is enough for the vehicle to pass through the intersection from the current vehicle position. For example, if the traffic signal is in red phase, the algorithm will determine whether the vehicle can stop before reaching the intersection based on the information about the current vehicle speed, the remaining red time, and the maximum deceleration rate of the vehicle. If the traffic signal is in green

phase, the algorithm will decide whether the vehicle will be able to pass through the intersection based on the information about the current vehicle speed, the remaining green time, and the maximum acceleration rate of the vehicle. If any of these two checks are not satisfied, the algorithm will stop the eco-driving trajectory planning and let the human driver determine the best course of action. On the other hand, if any of the two checks are satisfied, the real-time vehicle states information will be provided to the trained random forest model to determine the optimal speed at time *t*, after which the system will start the process for the next time step *t+1*.

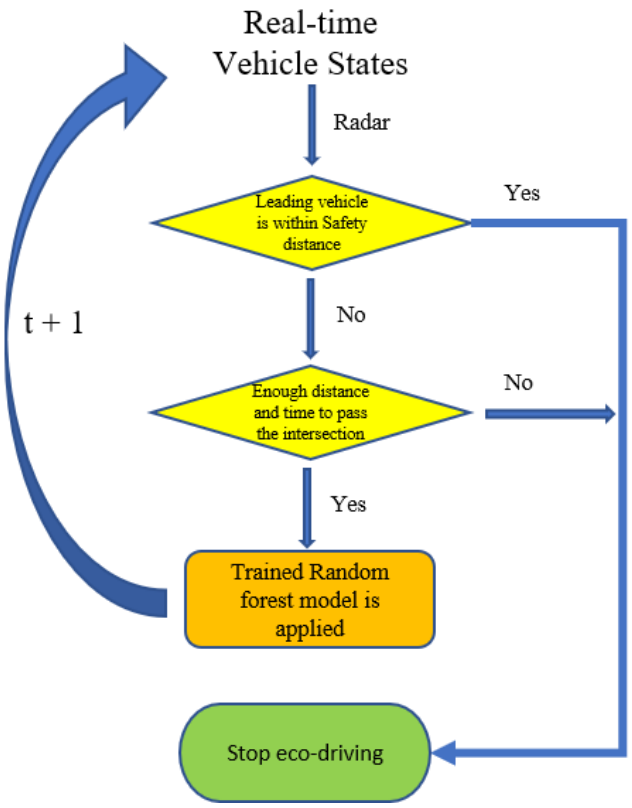

Figure 6.4 Online process of the BETEAD algorithm

6.5 Case Study and Results

6.5.1 Simulation Corridor Setup

To further validate the proposed algorithm and study the potential energy savings, we built and calibrated a simulation network with two signalized corridors based on the real-world traffic in the city of Carson, California. PTV VISSIM (*54*), a microscopic multi-modal traffic simulator, was used to evaluate the BETEAD algorithm in a simulation environment. A dynamic-link library (DLL) interface was developed to communicate between the VISSIM simulation environment and the BETEAD algorithm so that the equipped vehicles that are simulated in VISSIM can follow the optimal speed profile generated by the BETEAD algorithm. As shown in Figure 6.5, The 4.3-mile corridor on Alameda St has eight signalized intersections where five of which are connected. Each direction has 2-3 lanes with a speed limit of 45mph. On the west of Alameda St, another 3.3-mile corridor on Wilmington Ave has eleven signalized intersections with five connected. Each direction has 2 lanes with a speed limit of 40mph. While an electric truck could receive SPaT and conduct eco-driving at connected intersections, it will perform normal driving in the rest of the corridor. The traffic data and signal timing are calibrated using the real-world data in both directions.

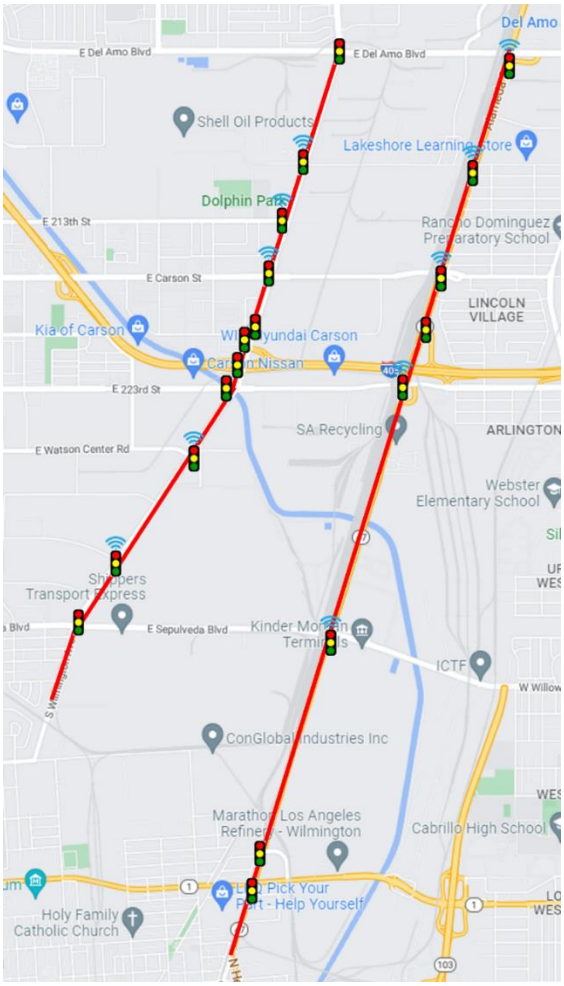

Figure 6.5 Simulation Corridors, Alameda St and Wilmington Ave in Carson, CA.

To further validate the proposed algorithm and study the potential energy savings, we built and calibrated a simulation network with two signalized corridors based on the real-world traffic in the city of Carson, California. PTV VISSIM [24], a microscopic multi-modal traffic simulator, was used to evaluate the BETEAD algorithm in a simulation environment. A dynamic-link library (DLL) interface was developed to communicate between the VISSIM simulation environment and the BETEAD algorithm so that the equipped vehicles that are simulated in VISSIM can follow the optimal speed profile generated by the

BETEAD algorithm. As shown in Figure 6.5 The 4.3-mile corridor on Alameda St has eight signalized intersections where five of which are connected. Each direction has 2-3 lanes with a speed limit of 45mph. On the west of Alameda St, another 3.3-mile corridor on Wilmington Ave has eleven signalized intersections with five connected. Each direction has 2 lanes with a speed limit of 40mph. While an electric truck could receive SPaT and conduct eco-driving at connected intersections, it will perform normal driving in the rest of the corridor. The traffic data and signal timing are calibrated using the real-world data in both directions.

6.5.2 Performance Comparison on Different Corridors and Intersections

For each corridor and direction, a host vehicle will perform eco-drive for a total of 100 simulations with different seed numbers to simulate a variety of circumstances. The travel time and electric energy consumption compared between the baseline and *BETEAD* is shown in Table 6.2.

As can be seen from Table 6.2, the electric energy of BETEAD in all four scenarios has shown savings ranging from 1.4% to 6.5%, with an average saving of 3.1%. While the travel time of the BETEAD truck is shorter than the baseline truck on Alameda St, it is longer on Wilmington Ave, mainly due to the shorter intersection spacing and heavier traffic. We split the electric energy into two parts, positive energy and regenerative braking energy, where the former is the energy consumed by accelerating and cruising, and the latter is the energy recovered through regenerative braking. As can be seen from the table, BETEAD consumes less positive energy on all four corridors, ranging from 4.8% to 12.1%, due to less acceleration and deceleration. Meanwhile, the more frequent hard braking in

the baseline truck create more regenerative braking energy for the electric truck,, ranging from 25.7% to 35.0%.

Table 6.2 Differences in Travel Time and Electric Energy Consumption of Host Vehicle between Baseline and BETEAD

Corridor/ Direction	BETEAD/ Baseline	Travel Time (s)	Electric Energy (10^6J)	Positive Energy (10^6J)	Regenerative Braking Energy(10^6J)
Alameda North	Baseline	622	57.3	65.5	-8.2
	BETEAD	620	56.3	62.4	-6.1
	Savings	0.2%	1.8%	4.8%	25.7%
Alameda South	Baseline	977	64.8	75.4	-11.1
	BETEAD	963	63.9	71.5	-7.6
	Savings	1.4%	1.4%	5.2%	31.1%
Wilmington North	Baseline	716	48.6	60.3	-11.6
	BETEAD	776	45.4	53.0	-7.5
	Savings	-8.5%	6.5%	12.1%	35.0%
Wilmington South	Baseline	992	54.0	64.1	-10.1
	BETEAD	1042	52.6	59.2	-6.6
	Savings	-5.1%	2.6%	7.7%	34.9%

Since the BETEAD truck will operate in the same way as the baseline truck at non-connected intersections, the energy savings will seem to be lower when averaging along the entire corridor. To better distinguish the performance of BETEAD at connected versus non-connected intersections, we define segments of vehicle trajectories associated with intersections as those within 750 meters upstream and 100 meters downstream of each intersection, and then analyze the travel time and electric energy consumption at the individual intersections. The results for the Alameda North corridor are shown in Table 6.3. The combined electric energy savings at all the five connected intersections is 6.8%, which confirms the energy savings benefit of the BETEAD algorithm.

Table 6.3 Differences in Travel Time and Electric Energy Consumption of Host Vehicle between Baseline and BETEAD for each Intersection in Alameda North

	Intersection	Connected	Travel Time (s)	Electric Energy (10^6 J)
Baseline	**1**	No	45	2.3
	2	No	48	6.2
	3	No	49	4.7
	4	No	49	4.9
	5	No	82	4.2
	6	No	29	3.8
	7	No	96	6.1
	8	No	70	6.0
BETEAD	**1**	No	45	2.3
	2	No	48	6.2
	3	Yes	47	4.6
	4	Yes	48	5.0
	5	No	82	4.7
	6	Yes	29	3.8
	7	Yes	101	4.9
	8	Yes	65	5.4
Total	**Baseline**	Yes	292	25.4
		No	175	12.7
	BETEAD	Yes	290	23.7
		No	175	13.2
	Savings	Yes	0.6%	6.8%
		No	0.0%	-4.1%

To visually illustrate how the electric truck could save energy while maintaining a similar travel time, we plot the speed profiles of all the simulation runs in baseline and BETEAD as shown in Figure 6.6 and Figure 6.7 along Alameda St Northbound and Wilmington Ave Northbound, respectively. Each intersection is labeled with red or green dotted line to indicate whether they are connected or non-connected and the average speed of each run is represented with a range of rainbow colors. Note that some runs (7% on average) with heavy oversaturation are not taken into account in the analysis. As can be seen from Figure 6.6(a), the electric truck performs a hard brake at each intersection. The BETEAD can adjust its speed 750 meters ahead the connected intersection to avoid stopping at red light. The comparison is most obvious at Dominguez St and Del Amo St, where the BETEAD achieves a smoother speed profile and saves electric energy, as shown in Figure 6.6(b). A similar trend can be seen from the BETEAD speed profiles in Figure 6.7 on Wilmington NB, which results in 6.5% energy savings. Compared to the baseline trajectories in 6.7(a) where vehicles often perform hard brakes at every intersection leading to full stops, the speed profiles of BETEAD in 6.7(b) show an early adjustment for all the connected intersections (colored in dotted green) and thus avoiding unnecessary acceleration and deceleration. It's also noteworthy that the travel time of the BETEAD trucks is unexpectedly 8.5% longer than the baseline. This is due to the fact that the spacing between intersections (223rd St, Ramp 405E, Ramp 405W, and 220th St) appears to be much smaller and the corridor is more congested, causing the Eco-Drive electric truck not able to reach the optimal cruising speed after passing each intersection.

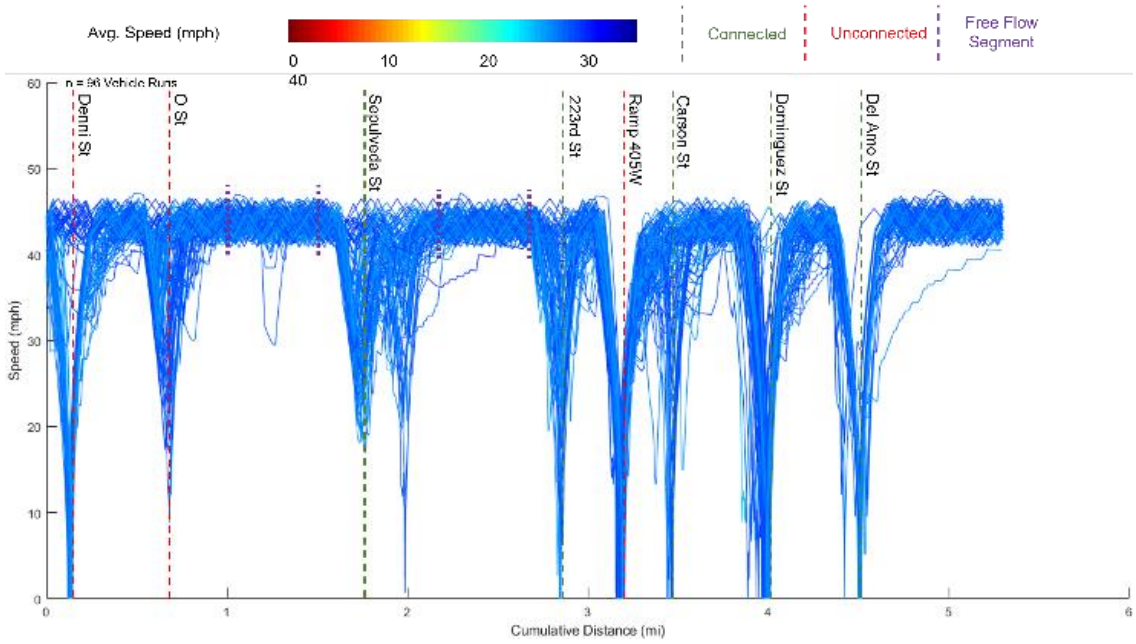

(a) Baseline

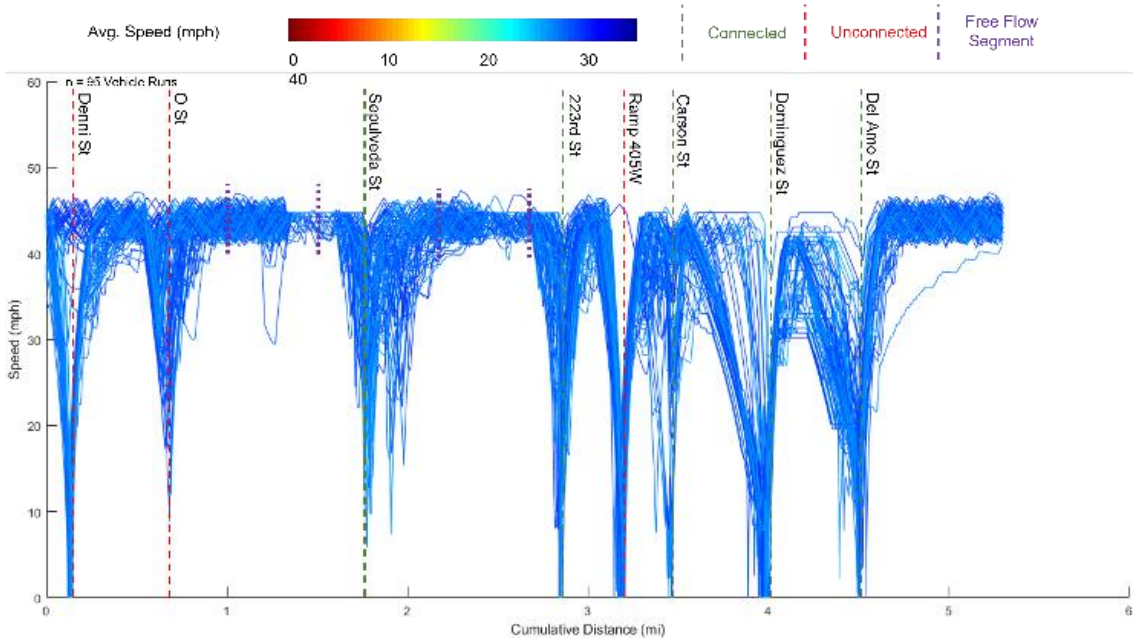

(b) BETEAD

Figure 6.6. Speed profiles of electric truck along Alameda St NB

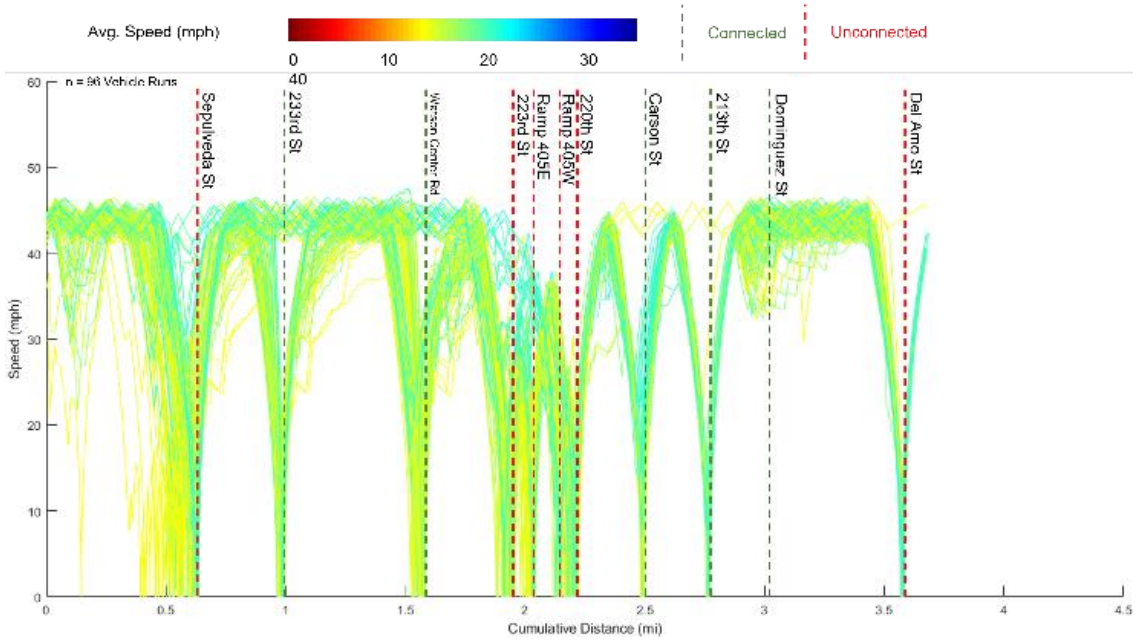

(a) Baseline

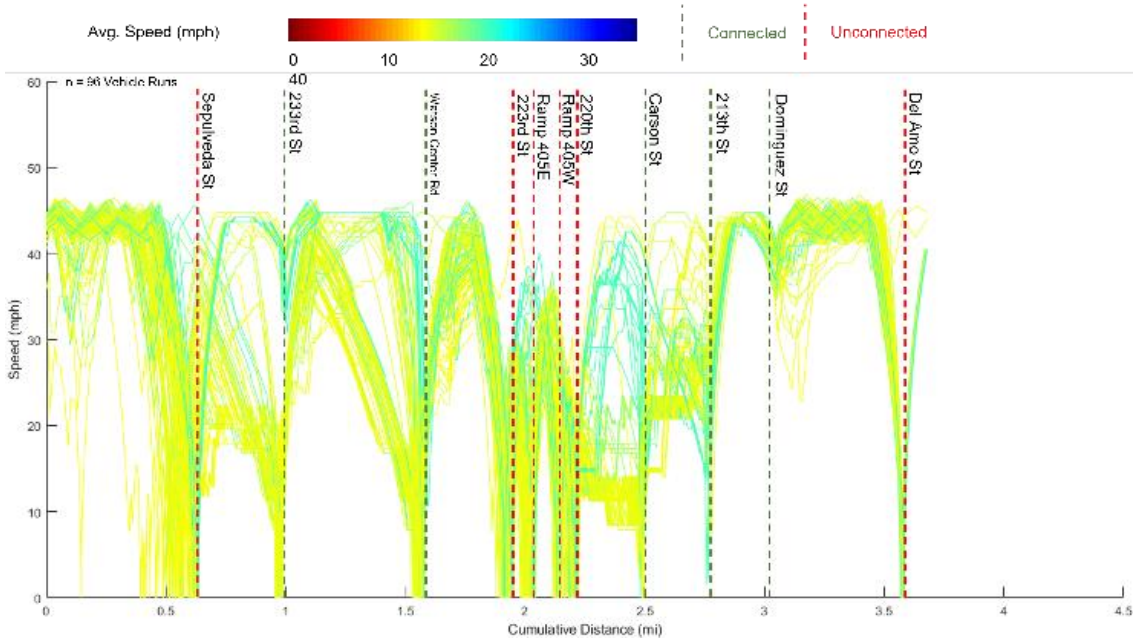

(b) BETEAD

Figure 6.7. Speed profiles of electric truck along Wilmington Ave NB

6.5.3 Comparison between Electric Truck and Diesel Truck

We notice that the electric truck energy saving percentage appears to be smaller than the savings of diesel trucks (3.1% to 10.8%) based on the authors' previous research (*24*). To compare the different driving behaviors between baseline, diesel eco-drive truck, and electric eco-drive truck, we run the simulations of different vehicles using the same 100 seeds to ensure the vehicles have the same initial conditions. According to the simulation results, one of the reasons is due to the higher energy consumption percentage of free flow in the trip of electric trucks compared to diesel trucks. We calculate the energy of free flow in the two 0.5-mile segments shown in Figure 6.9 (between labeled purple segments), and the electric trucks take an average share of 16.61% of the trip total energy while diesel trucks only take an average share of 15.66%. Since the energy saving is mainly introduced in the acceleration & deceleration period, the lower energy share of the speed changing segments for electric trucks will cause the energy saving to be smaller than diesel trucks.

The other reason is the regenerative braking capability of electric trucks that could generate energy while braking in front of intersections and compensate part of the energy needed to accelerate to cruising speed. As can be seen from the histogram plot of acceleration in Figure 6.8, both the diesel and electric eco truck appears to have lower acceleration frequencies at [-2, -1.8] mph/s and [0.4, 0.6] mph/s, and much higher mild deceleration frequency at [-0.6, 0.4] mph/s compared to baseline, resulting in more comfortable driving experience and less waiting at intersections. The electric eco-drive truck has a slightly higher frequency of decelerating at [-1.2, -1] mph/s than eco diesel truck due to the

regenerative braking function and the BETEAD algorithm generates the trajectory with slightly more decelerations.

To show that each type of truck has a unique eco-friendly trajectory customized by its own powertrain, we plot the sample trajectories between two types of eco vehicles in Figure 6.9. Under the same initial condition, the eco-drive trajectory designed for electric truck prefers a relatively aggressive accelerating and decelerating strategy starting from the first connected intersection, while the eco-drive trajectory designed for diesel truck prefers slow deceleration pattern, as highlighted with red circle. If a diesel truck follows the eco-drive trajectory designed for electric truck, the mismatched plan will cause 12.2% additional energy consumption. On the other hand, if an electric truck follows the eco-drive trajectory designed for diesel truck, the mismatched plan will cause 10.2% additional energy consumption. This comparison shows that an EAD plan designed specific to the type and powertrain of the vehicle would maximize the energy benefit of truck eco-drive.

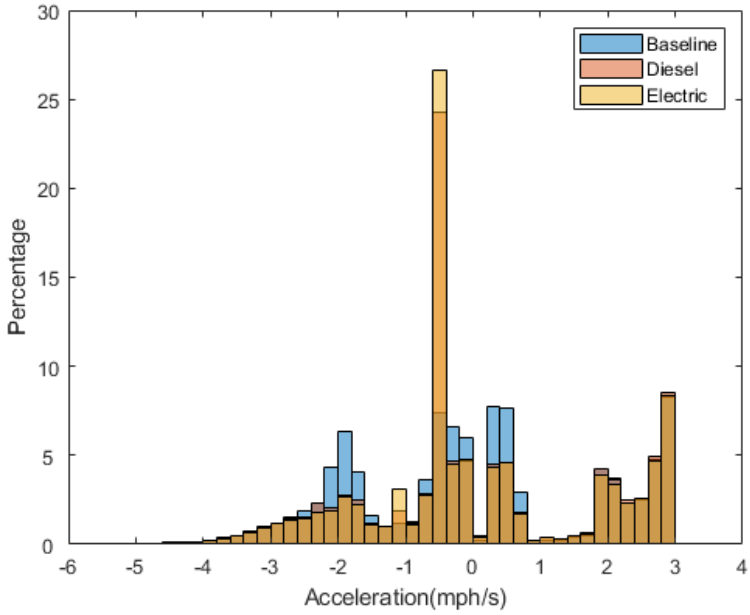

Figure 6.8. Comparison of histogram of acceleration frequency between baseline, eco diesel truck and eco electric truck at Wilmington Ave SB.

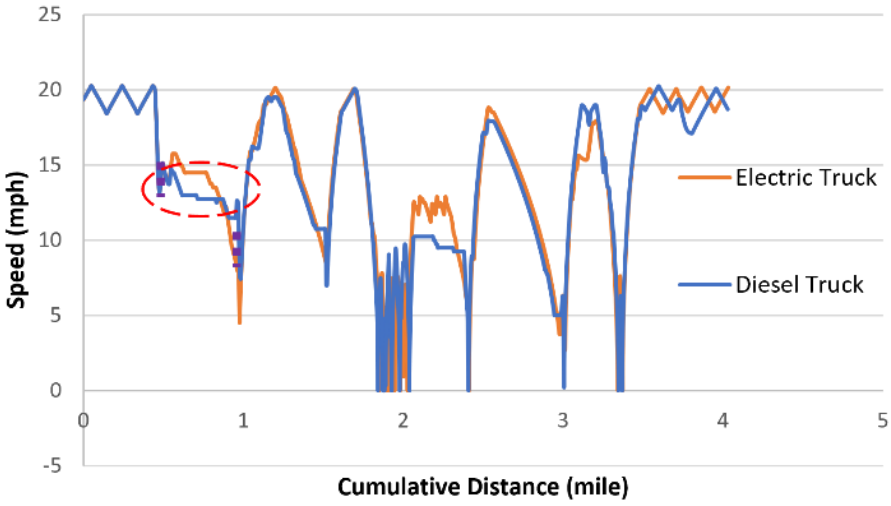

Figure 6.9. Comparison of trajectory between eco diesel truck and eco electric truck from the same seed of run at Wilmington Ave SB.

6.6 Summary and Discussion

This chapter presented an EAD algorithm for BETs approaching pre-timed signalized intersections in an energy-efficient manner. A machine learning model is trained to

generate an approximate solution from the graph-based model in order to reduce computation time for real-time calculation. The evaluation results from microscopic traffic simulation show that the BETEAD algorithm could help the host vehicle achieve an energy savings of 1.4% to 6.5% on different simulation corridors. In addition, the BET energy consumption and travel time are compared at the intersection-level to better distinguish the performance of BETEAD at connected versus non-connected intersections. The results show that the combined electric energy savings at the connected intersections is 6.8%, confirming the energy savings benefit of the BETEAD algorithm. The comparison between diesel trucks and BETs that use the EAD algorithm shows that the BETs would benefit relatively less from EAD in terms of energy savings due to their regenerative braking capability, but they would still gain the same level of benefit in terms of driving comfort.

7. Conclusions and Future Work

7.1 Conclusions

This dissertation has presented a variety of connected eco-driving algorithms to adapt to the dynamic and uncertain traffic and signal conditions. These algorithms are also applicable to different types and models of vehicles in both intersection and corridor-based environments, proved with evaluation results from either microscopic simulation or real-world data. Specifically, the dissertation has made the following contributions:

1) We designed a comprehensive framework for adaptive connected eco-driving strategy under mixed traffic conditions. The framework was tested with different types of vehicles, upcoming traffic, and signal information for both energy consumption and mobility. Numerical simulations have shown that the proposed method is robust and adaptive to varying traffic and queue conditions, and could achieve around 9% energy savings compared to other baseline methods.
2) We proposed a learning-based model for efficient computation. This model was trained on existed/developed optimization methods using collected historical traffic data to guarantee optimality. The simulation results tested on BETs show that the proposed EAD algorithm could achieve an energy savings of 1.4% to 6.5% while achieving faster computational time and maintaining a similar travel time under different simulation environments.
3) We extended the traditional EAD algorithm for corridor-level optimization. The algorithm could reach global minimum of expected energy consumption using inputs of all the SPaT data from the signal controllers in downstream, achieving an

energy savings of 8.8% - 11.8% for the case when two intersections are 400m aparted, and 16.3% - 27.8% for the closely spaced intersections.

7.2 Selected Publications

Below are some publications resulted from the author's research work:

1. Wei, Z., Hao, P., & Barth, M., "Developing an Adaptive Strategy for Connected Eco-Driving under Uncertain Traffic Condition," 2019 IEEE Intelligent Vehicles Symposium (IV), Paris, France, 2019, pp. 2066-2071, doi: 10.1109/IVS.2019.8813819.

2. Wei, Z., Hao, P., Barth, M., & Boriboonsomsin, K. (2022). Evaluating Contraflow High-Occupancy Vehicle Lane Designs for Mitigating High-Occupancy Vehicle Lane Performance Degradation. Transportation Research Record, 03611981221135805.

3. Wei, Z., Wang, C., Hao, P., & Barth, M. J. (2019, October). Vision-based lane-changing behavior detection using deep residual neural network. In 2019 IEEE Intelligent Transportation Systems Conference (Wei, Z., Jiang, Y., Liao, X., Qi, X., Wang, Z., Wu, G., ... & Barth, M. (2020). 4. End-to-end vision-based adaptive cruise control (ACC) using deep reinforcement learning. arXiv preprint arXiv:2001.09181.ITSC) (pp. 3108-3113). IEEE.

5. Hao, P., Wei, Z., Esaid, D., Williams, N., Kailas, A., Amar, P., ... & Boriboonsomsin, K. (2021, September). Connected Vehicle-based Truck Eco-Driving: A Simulation Study. In 2021 IEEE International Intelligent Transportation Systems Conference (ITSC) (pp. 1592-1597). IEEE.

6. Wei, Z., Qi, X., Bai, Z., Wu, G., Nayak, S., Hao, P., ... & Oguchi, K. (2022, June).

Spatiotemporal Transformer Attention Network for 3D Voxel Level Joint Segmentation and Motion Prediction in Point Cloud. In 2022 IEEE Intelligent Vehicles Symposium (IV) (pp. 1381-1386). IEEE.

7.3 Future Work

Although many connected eco-driving algorithms have been presented in this dissertation, there are still some directions that could be explored based on the presented work:

- Combine cooperativity and the developed single-vehicle targeted eco-driving algorithms. It is expected that when the percentage of vehicles equipped with currently developed eco-driving systems, the energy-saving effect might reduce due to the non-cooperative driving behavior of the algorithm. Energy efficiency is expected to be further improved with the help of vehicle cooperation and platooning.
- Consider more interactions between the host vehicle and its surrounding nonconnected vehicles. For example, when a nonconnected vehicle overtakes the host vehicle near the intersection, the previously designed trajectory has to be adjusted based on the new situation. These kinds of behaviors could be predicted based on the collected information and improve the energy efficiency of the trajectory.
- Consider trajectory planning algorithms with lateral control strategies. With appropriate lane change strategies, the duration of eco-driving could be extended as well as the travel time could be reduced. For example, when a front vehicle has

been detected and could potentially affect the switch of eco-driving, it could wisely choose another lane with less traffic and extend the duration of eco-driving.

- Conduct more field tests in established connected vehicle testbeds. With real-world field tests, the proposed method could be fully tested in terms of safety, mobility, and energy efficiency for future improvements.

Bibliography

1. U.S. Department of Energy, “Transportation energy data book”, https://www.epa.gov/system/files/documents/2023-04/US-GHG-Inventory-2023-Main-Text.pdf

2. U.S. Energy Consumption by the Transportation Sector | Bureau of TransportationStatistics.https://www.bts.gov/content/us-energy-consumptiontransportation-sector

3. California Public Utilities Commission, “Zero-Emission Vehicles”, [Online]. Available: [Accessed: July -2020].

4. Lee, J. and B. Park, Development and evaluation of a cooperative vehicle intersection control algorithm under the connected vehicles environment. IEEE Transactions on Intelligent Transportation Systems, Vol. 13, No. 1, 2012, pp. 81–90.

5. European Commission (EC), “eCoMove – Cooperative Mobility Systems and Services for Energy Efficiency”, http://www.ecomove-project.eu/. Jan. 2019.

6. U.S. Department of Transportation, “Applications for the Environment: Real-Time Information Synthesis (AERIS)”,

7. Ye, F., P. Hao, X. Qi, G. Wu, K. Boriboonsomsin, and M. J. Barth. Prediction-Based Eco-Approach and Departure at Signalized Intersections With Speed Forecasting on Preceding Vehicles. *IEEE Transactions on Intelligent Transportation Systems*, 2018.

8. Hao, P., G. Wu, K. Boriboonsomsin, and M. J. Barth. Eco-Approach and Departure (EAD) Application for Actuated Signals in Real-World Traffic. *IEEE Transactions on Intelligent Transportation Systems*, 2018.

9. Barth, M., S. Mandava, K. Boriboonsomsin, and H. Xia. Dynamic ECO-Driving for Arterial Corridors. 2011.

10. Eco-Approach and Departure at Signalized Intersections: Field Study and Modeling. 2013.

11. Hao, P., K. Boriboonsomsin, C. Wang, G. Wu, and M. Barth. Connected Eco-Approach and Departure (EAD) System for Diesel Trucks. 2018.

12. Li, M., K. Boriboonsomsin, G. Wu, W.-B. Zhang, and M. Barth. Traffic Energy and Emission Reductions at Signalized Intersections: A Study of the Benefits of Advanced

Driver Information. *International Journal of Intelligent Transportation Systems Research*, Vol. 7, No. 1, 2009.

13. Asadi, B., and A. Vahidi. *Predictive Use of Traffic Signal State for Fuel Saving*. IFAC, 2009.

14. Hao, P., G. Wu, K. Boriboonsomsin, and M. J. Barth. Developing a Framework of Eco-Approach and Departure Application for Actuated Signal Control. *IEEE Intelligent Vehicles Symposium, Proceedings*, 2015.

15. Mandava, S., K. Boriboonsomsin, and M. Barth. Arterial Velocity Planning Based on Traffic Signal Information under Light Traffic Conditions. *IEEE Conference on Intelligent Transportation Systems, Proceedings, ITSC*, 2009, pp. 160–165.

16. Rakha, H., and R. Kamalanathsharma. Eco-Driving at Signalized Intersections Using V2I Communication. *IEEE Conference on Intelligent Transportation Systems, Proceedings, ITSC*, 2011, pp. 341–346.

17. Kamalanathsharma, R., and H. Rakha. Multi-Stage Dynamic Programming Algorithm for Eco-Speed Control at Traffic Signalized Intersections. *IEEE Conference on Intelligent Transportation Systems, Proceedings, ITSC*, 2013.

18. De Nunzio, G., C. Canudas de Wit, P. Moulin, and D. Di Domenico. Eco-Driving in Urban Traffic Networks Using Traffic Signals Information. *International Journal of Robust and Nonlinear Control*, Vol. 26, No. 6, 2015.

19. Mahler, G., and A. Vahidi. An Optimal Velocity-Planning Scheme for Vehicle Energy Efficiency through Probabilistic Prediction of Traffic-Signal Timing. *IEEE Transactions on Intelligent Transportation Systems*, Vol. 15, No. 6, 2014, pp. 2516–2523.

20. G. Wu et al., "Eco-approach and departure along signalized corridors considering powertrain characteristics," SAE Int. J. Sustain. Transp., Energy, Environ., Policy, vol. 2, no. 1, pp. 1–16, Mar. 2021.

21. Jin, Q., G. Wu, K. Boriboonsomsin, and M. J. Barth. Power-Based Optimal Longitudinal Control for a Connected Eco-Driving System. *IEEE Transactions on Intelligent*

22. Y. Fei, P. Hao, X. Qi, G. Wu, K. Boriboonsomsin, and M. Barth, "Prediction-based eco-approach and departure strategy in congested urban traffic". Proceedings of the 96th Annual Meeting of Transportation Research Board, Washington, DC. 2017.

23. Lu, Shaofeng, Fei Xue, Tiew On Ting, and Yang Du. "Speed trajectory optimisation for electric vehicles in eco-approach and departure using linear programming." (2016): 12-6.

24. Hao, Peng, Zhensong Wei, Danial Esaid, Nigel Williams, Aravind Kailas, Pascal Amar, Kyle Palmeter et al. "Connected Vehicle-based Truck Eco-Driving: A Simulation Study." In 2021 IEEE International Intelligent Transportation Systems Conference (ITSC), pp. 1592-1597. IEEE, 2021.

25. Altan, Osman D., Guoyuan Wu, Matthew J. Barth, Kanok Boriboonsomsin, and John A. Stark. "GlidePath: Eco-friendly automated approach and departure at signalized intersections." IEEE Transactions on Intelligent Vehicles 2, no. 4 (2017): 266-277.

26. Jiang, Huifu, Shi An, Jian Wang, and Jianxun Cui. "Eco-approach and departure system for left-turn vehicles at a fixed-time signalized intersection." Sustainability 10, no. 1 (2018): 273.

27. Ye, Fei, Peng Hao, Guoyuan Wu, Danial Esaid, Kanok Boriboonsomsin, Zhiming Gao, Tim LaClair, and Matthew Barth. Deep learning-based queue-aware eco-approach and departure system for plug-in hybrid electric buses at signalized intersections: a simulation study. Oak Ridge National Lab.(ORNL), Oak Ridge, TN (United States), 2020.

28. Guo, Lulu, Bingzhao Gao, Ying Gao, and Hong Chen. "Optimal energy management for HEVs in eco-driving applications using bi-level MPC." IEEE Transactions on Intelligent Transportation Systems 18, no. 8 (2016): 2153-2162.

29. Wan, Nianfeng, Ardalan Vahidi, and Andre Luckow. "Optimal speed advisory for connected vehicles in arterial roads and the impact on mixed traffic." Transportation Research Part C: Emerging Technologies 69 (2016): 548-563.

30. Jiang, Huifu, Jia Hu, Shi An, Meng Wang, and Byungkyu Brian Park. "Eco approaching at an isolated signalized intersection under partially connected and automated vehicles environment." Transportation Research Part C: Emerging Technologies 79 (2017): 290-307.

31. He, Xiaozheng, Henry X. Liu, and Xiaobo Liu. "Optimal vehicle speed trajectory on a signalized arterial with consideration of queue." Transportation Research Part C: Emerging Technologies 61 (2015): 106-120.

32. Qi X, Barth MJ, Wu G, Boriboonsomsin K, Wang P. Energy impact of connected eco-driving on electric vehicles. In Road Vehicle Automation 4 2018 (pp. 97-111). Springer, Cham.

33. Z. Bai, P. Hao, W. ShangGuan, B. Cai and M. J. Barth, "Hybrid Reinforcement Learning-Based Eco-Driving Strategy for Connected and Automated Vehicles at Signalized Intersections,"

34. Z. Wang et al., “Early Findings from Field Trials of Heavy-Duty Truck Connected Eco-Driving System,” 2019 IEEE Intelligent Transportation Systems Conference (ITSC), Auckland, New Zealand, pp. 3037-3042

35. P. Hao, K. Boriboonsomsin, G. Wu, Z. Gao, T. LaClair and M. Barth “Deeply Integrated Vehicle Dynamic and Powertrain Operation for Efficient Plug-in Hybrid Electric Bus,” *Proceedings of the 98th Annual Meeting of Transportation Research Board*, Washington, DC, 2019.

36. Zhang, Jian, Xia Jiang, Suping Cui, Can Yang, and Bin Ran. "Navigating Electric Vehicles Along a Signalized Corridor via Reinforcement Learning: Toward Adaptive Eco-Driving Control." Transportation Research Record (2022): 03611981221084683.

37. Li, Weixia, Guoyuan Wu, Matthew J. Barth, and Yi Zhang. "Safety, mobility and environmental sustainability of eco-approach and departure application at signalized intersections: A simulation study." In 2016 IEEE Intelligent Vehicles Symposium (IV), pp. 1109-1114. IEEE, 2016.

38. Asadi, Behrang, and Ardalan Vahidi. "Predictive cruise control: Utilizing upcoming traffic signal information for improving fuel economy and reducing trip time." IEEE transactions on control systems technology 19, no. 3 (2010): 707-714.

39. Li, Weixia, Guoyuan Wu, Yi Zhang, and Matthew J. Barth. "Safety analysis of the eco-approach and departure application at a signalized corridor." Tsinghua Science and Technology 23, no. 2 (2018): 157-171.

40. Han, Jihun, Dominik Karbowski, and Aymeric Rousseau. "State-Constrained Optimal Solutions for Safe Eco-Approach and Departure at Signalized Intersections." In Dynamic Systems and Control Conference, vol. 84270, p. V001T10A001. American Society of Mechanical Engineers, 2020.

41. Sun, Chao, Xinwei Shen, and Scott Moura. "Robust optimal eco-driving control with uncertain traffic signal timing." In 2018 annual American control conference (ACC), pp. 5548-5553. IEEE, 2018.

42. Ozatay, Engin, Umit Ozguner, Dimitar Filev, and John Michelini. "Analytical and numerical solutions for energy minimization of road vehicles with the existence of multiple traffic lights." In 52nd IEEE conference on decision and control, pp. 7137-7142. IEEE, 2013.

43. Lin, Qingfeng, Xuejin Du, Shengbo Eben Li, and Zhennan Ye. "Vehicle-to-infrastructure communication based eco-driving operation at multiple signalized intersections." In 2016 IEEE Vehicle Power and Propulsion Conference (VPPC), pp. 1-6. IEEE, 2016.

44. De Nunzio, Giovanni, Carlos Canudas De Wit, Philippe Moulin, and Domenico Di Domenico. "Eco-driving in urban traffic networks using traffic signals information." International Journal of Robust and Nonlinear Control 26, no. 6 (2016): 1307-1324.

45. Zhao, Xiangmo, Xia Wu, Qi Xin, Kang Sun, and Shaowei Yu. "Dynamic eco-driving on signalized arterial corridors during the green phase for the connected vehicles." Journal of Advanced Transportation 2020 (2020).

46. Yang, Hao, Fawaz Almutairi, and Hesham Rakha. "Eco-driving at signalized intersections: A multiple signal optimization approach." IEEE Transactions on Intelligent Transportation Systems 22, no. 5 (2020): 2943-2955.

47. Economics and Industry Data. (n.d.). Retrieved October 24, 2022, from https://www.trucking.org/economics-and-industry-data

48. U.S. Environmental Protection Agency (EPA), “Fast Facts: U.S. Transportation Sector GHG Emissions 1990-2020”, [Online]. Available: https://nepis.epa.gov/Exe/ZyPDF.cgi?Dockey=P10153PC.pdf. [Accessed: Oct -2022].

49. Adler, Alan (8 March 2019). "2019 Work Truck Show: Adoption of Electrification Won't be Fast". Trucks.com. Retrieved July 25, 2019.

50. Savković, Tatjana, Milica Miličić, Pavle Pitka, Ivana Milenković, and Dejan Koleška. "Evaluation of the eco-driving training of professional truck drivers." Operational Research in Engineering Sciences: Theory and Applications 2, no. 1 (2019): 15-26.

51. Hauenstein, J., Mertens, J.C., Diermeyer, F. and Zimmermann, A., 2021. Cooperative-and Eco-Driving: Impact on Fuel Consumption for Heavy Trucks on Hills. Electronics, 10(19), p.2373.

52. Wood SN. Thin plate regression splines. 2003. Journal of the Royal Statistical Society: Series B (Statistical Methodology). 65(1):95-114.

53. Esaid, D., Hao, P., Wu, G., Fei, Y., Wei, Z., Boriboonsomsin, K, Barth, M. (2021). Machine learning-based Eco-Approach and Departure: real-time trajectory optimization at connected signalized intersections. SAE International Journal of Sustainable Transportation, Energy, Environment, & Policy. 3(1):2021.

54. PTV Vissim Group. https://www.ptvgroup.com/en/solutions/products/ptv-vissim

55. Konstantinou, T., Gkritza, K., 2023a. Examining the barriers to electric truck adoption as a system: a Grey-DEMATEL approach. Transp. Res. Interdiscip. Perspect. 17, 100746 https://doi.org/10.1016/j.trip.2022.100746.

56. Tanvir, S.; Un-Noor, F.; Boriboonsomsin, K.; Gao, Z. Feasibility of Operating a Heavy-Duty Battery Electric Truck Fleet for Drayage Applications. Transp. Res. Rec. 2020, 2675, 258–268.

57. Stevanovic, Aleksandar, Jelka Stevanovic, and Cameron Kergaye. "Green light optimized speed advisory systems: Impact of signal phasing information accuracy." Transportation research record 2390.1 (2013): 53-59.

58. Saldivar-Carranza, Enrique, et al. Effects of a Probability-Based Green Light Optimized Speed Advisory on Dilemma Zone Exposure. No. 2020-01-0116. SAE Technical Paper, 2020.